Laboratory and Clinical Profile of

Alcohol-Induced Liver Fibrosis in a Transgenic Porcine Model

BY

NASYA MENDOZA-ELIAS
B.S., University of Chicago, 2012
M.D., University of Illinois at Chicago, 2018

THESIS

Submitted as partial fulfillment of the requirements
for the degree of Master of Science in Clinical and Translational Science
in the Graduate College of the
University of Illinois at Chicago, 2018

Chicago, Illinois

Defense Committee:

Ron Gaba, Advisor
Lawrence Shook, Nutritional Sciences
Jack Zwanziger, Chair

I would like to dedicate this manuscript to my mother, Dr. Magda Elias, and grandmother, Amanda Elias, whose strength, hard work, and emphasis on education and knowledge set the foundation for my pursuit of medicine and clinical science.

ACKNOWLEDGEMENTS

I would like to thank my family, friends, and mentors for their support and patience in completing this research project. I owe my success to them, associated research groups, and countless others who contributed to my edification.

In particular, I would like to thank Dr. Ron Gaba for his mentorship, guidance, and endless support over the past 2 years that made this project possible. Through his mentorship, he taught me that there is no replacement for well-executed science. Through his support, including his Interventional Radiology Fellowship, I was welcomed into a superb research team while working on this project and learned first-hand knowledge about the many moving parts in clinical translational research.

I would also like to thank the section of Interventional Radiology for being so welcoming and teaching me the nuances of general interventional radiology, liver disease and management, and encouragement throughout this process.

I would like to mention Dr. Lawrence Schook, who contributed substantially to my education through his previous work, current projects, and made the research fun through his pleasant, cooperative, and energetic personality.

I would like to mention Dr. Jack Zwanziger, who contributed to my instruction by providing guidance on project content and direction.

I would also like to thank Dr. Dan Regan at Colorado State University, whose veterinary pathology expertise made this project possible.

I would also like to thank the UIC Biological Resource Laboratory (BRL) for their support in caring for, monitoring, and ensuring general well-being of our animal subjects, without which it would not have been possible to complete this project.

TABLE OF CONTENTS

CHAPTER **PAGE**

I. INTRODUCTION 1

a. Background 1

i. Liver Fibrosis in Human Liver Disease 1

ii. Relevant Epidemiology 9

iii. Use of Oncopig Model in a Swine Model of Liver Fibrosis 11

b. Related Literature 12

i. Social Cost of Liver Disease 12

ii. Liver Disease models 13

c. Purpose of Study 15

d. Significance of Study 16

II. RESEARCH QUESTION 18

a. Approach to Research Question 18

b. Conceptual Framework 18

III. METHODS 20

a. Study Design 20

b. Timeline 22

i. Animal Care 24

ii. Serum Laboratory Collection 24

iii. Clinical Assessment 25

c. Fibrosis Induction Procedure 26

d. Biopsy Procedure 27

i. Laboratory Values 28

e. Tissue Processing 31

i. Sample Collection 31

ii. Histology Core Preparation of Slides 31

f. Histology Assessment 31

i. Pathologic Assessment of Slides Utilizing Porcine Fibrosis and Inflammation Scoring System 32

g. Statistical Methods 33

i. Vital Signs and Body Measurement Statistical Analysis 33

ii. Laboratory Statistical Analysis 34

iii. Histological Statistical Analysis 34

h. Overall Evaluation of Fibrosis 34

TABLE OF CONTENTS (continued)

IV. RESULTS 36
a. Procedure Results 36
i. Average Dose Administered 36
ii. Size, Flow, and Anatomic Site of Infiltration 36
b. Laboratory values 37
i. Vitals and Body Measurements 37
ii. Complete Metabolic Panel 40
iii. Complete Blood Count 42
iv. Coagulation Profile 44
v. Liver Function Profile 45
c. Histological Outcome 50
d. Clinical Impact 54

V. DISCUSSION 58
a. Outcome of Fibrosis Induction 58
i. Procedure Outcome 58
ii. Possible Variations in Procedure 60
iii. Clinical Outcome: Interpretation of Outcome Measures 60
b. Importance as Background in Developing Cancer Model of HCC 63

CONCLUSION 64

CITED LITERATURE 69

VITA 74

LIST OF TABLES

TABLE **PAGE**

I SUMMARY TABLE OF ANIMAL MODELS OF PORTAL HYPERTENSION AND LIVER FIBROSIS 17

II SWINE MODIFIED METAVIR FIBROSIS GRADING SCHEME 32

III SWINE MODIFIED METAVIR INFLAMMATION GRADING SCHEME 33

IV VOLUME OF INFUSED LIPIODOL:ETHANOL EMULSION ADMINISTERED PER ANIMAL IN BOTH COHORTS AND CONTROL GROUP 37

V BODY MEASUREMENTS ACROSS GROUPS. 39

VI COMPLETE METABOLIC PANEL OF ALL COHORTS 41

VII COMPLETE BLOOD COUNT OF ALL COHORTS. 43

VIII COAGULATION PROFILE OF ALL COHORTS. 45

IX LIVER FUNCTION PROFILE OF ALL COHORTS. 46

X HISTOPATHOLOGICAL OUTCOME: PERCENT FIBROSIS, METAVIR FIBROSIS SCORE, METAVIR INFLAMMATION SCORE 502

XI COHORT 1 LIVER HISTOLOGICAL ASSESSMENT 53

XII COHORT 2 LIVER HISTOLOGICAL OUTCOMES 53

LIST OF FIGURES

FIGURE **PAGE**

Figure 1 Conceptual framework for a swine model of fibrosis induction. 19

Figure 2 Anatomic diagram of hepatic circulation. 21

Figure 3 Control Cohort: Time Course for Comparison of Disease Course. 21

Figure 4 Cohort 1: Validation of Fibrosis Induction Time Course. 23

Figure 5 Cohort 2: Extended Time Course for Study of Disease Course. 24

Figure 6 Representative images from fibrosis induction procedure. 28

Figure 7 Representative images from fibrosis induction procedure. 29

Figure 8 Representative images from fibrosis induction procedure. 30

Figure 9 Gross histology of cohort 1. 54

Figure 10 Representative images of Masson's trichrome stain in cohort 2. 55

Figure 11 Representative images of Masson's trichrome stain in cohort 1. 55

Figure 12 Representative images of Masson's trichrome stain in cohort 1 56

Figure 13 Representative images of Masson's trichrome stain in cohort 2 57

LIST OF ABBREVIATIONS

AALAC	Assessment and Accreditation of Laboratory Animal Care
ADH	Antidiuretic Hormone
ALD	Alcohol Liver Disease
ALT	Alanine Aminostransferase
AST	Aspartate Aminotransferase
BUN	Blood Urea Nitrogen
CBC	Complete Blood Count
CCl_4	Carbon Tetrachloride
CDAA	Choline-Deficient L-Amino Acid Diet
CSPH	Clinically Significant Portal Hypertension
DEN	Diethylnitrosamine
DMNA	Dimethylnitroasmine
GGT	Gamma-Glutamyl Transferase
HCC	Hepatocellular Carcinoma
HVPG	Hepatic Venous Pressure Gradient
IACUC	Institutional Animal Care and Use Committee
INR	International Normalized Ration
KRASG12D	Mutation notation
NAFLD	Non-Alcoholic Fatty Liver Disease
NASH	Non-Alcoholic Steatohepatitis
OCM	Oncopig Model
PH	Portal Hypertension
PT	Prothrombin Time
PTT	Partial Thromboplastin Time
TAA	Thioacetamide

LIST OF ABBREVIATIONS (continued)

TERT	Telomerase Reverse Transcriptase
TP53R167H	Mutation notation

SUMMARY

Liver disease affects ten percent of the world's population, and estimates show that this yearly incidence is growing each year. Liver fibrosis is a key point in the progression of alcohol liver disease, as it represents the point at which liver damage is no longer reversible and treatment algorithms shift towards more expensive treatment aimed at controlling symptoms of liver damage rather than reversing liver damage. Additionally, fibrosis progresses to cirrhosis, which in turn progresses to hepatocellular carcinoma. Alcohol liver disease is responsible for approximately ninety percent of hepatocellular carcinoma cases, an expensive disease to treat with an uncomfortable quality of life for patients. Therefore, a large animal model of alcohol-induced liver fibrosis is key in research development of clinically relevant medical and interventional treatments for end-stage liver disease and also for hepatocellular carcinoma.

This study aims to create a large animal model of liver fibrosis in the oncopig model. The oncopig is a transgenic swine with heterozygous KRAS and TP53 mutations that are present in over fifty percent of gastric cancers, which will be key in creating a hepatocellular carcinoma model. Fibrosis induction procedure was performed in two experimental cohorts of five oncopigs, one serially monitored for eight weeks after fibrosis induction and an extended cohort serially monitored for twenty weeks after fibrosis induction. Both experimental cohorts were compared to the control group in three main areas: clinical exam including neurological assessment, serological biomarkers, and histological assessment for fibrosis and inflammation. Statistical analysis for continuous variables was done using a two-tailed t-test, and for categorical variables was done using one-way ANOVA.

Fibrosis induction procedure was successful in all ten animals, with peak fibrosis of F3 reached at two to three weeks, but not persistent at twenty weeks. There were no significant differences in neurological assessment or serological biomarkers.

This study shows that fibrosis induction procedure is successful in inducing fibrosis at two to three weeks post-induction, indicating a regeneration and resolution of fibrosis and inflammation. This is analogous to the natural disease course of alcohol liver disease in humans, which only develops after chronic misuse of alcohol, equating to contrasting periods of ethanol intoxication and liver damage reversal until liver damage reaches liver fibrosis. This is an important step in creating a persistent large animal model of liver fibrosis in a transgenic swine with utility in translational studies for medical and interventional treatment.

I. INTRODUCTION

Worldwide, about 10% of the world's population suffers from liver disease(Yang 2008; Sofair et al. 2010). Liver disease is one of the top 20 causes of death in both developing and developed countries. In the United States, 1 in 10 adults suffers from liver disease with over 100 causes of liver disease. Because alcohol liver disease often progresses to hepatocellular carcinoma, an expensive disease to treat with healthcare and social cost totaling to 1.6% of US Gross Domestic Product(Mohapatra et al. 2010), it is of interest to create both an animal model that both follows the same disease course seen humans and also has a natural history of disease course that is analogous to that of humans.

a. Background

This section will summarize normal liver function in the human, what cirrhosis and fibrosis means in human disease, what measures are used to diagnosis and monitor cirrhosis, the epidemiology of cirrhotic liver disease in public health, and the Oncopig Model (OCM) and its relevance to this project. This background will aid in understanding the necessity of a large animal model for liver fibrosis and specifically, why the OCM is ideal for studying the natural course of liver disease from mild liver disease to cancerous progression.

i. Liver Fibrosis in Human Liver Disease

This section will review liver fibrosis as it occurs in human liver disease. The purpose of this section is to define both normal liver function and the natural history of liver disease as it progresses from mild to severe, and where liver fibrosis should be considered on this continuum. This section will also place into perspective how much of this liver disease continuum is captured by a model of liver fibrosis in the OCM, further explaining this project's relevance and utility.

In the normal liver, a sinusoidal micro-architecture facilitates the inflow of systemic venous blood through the peripherally located portal triad, (branch of portal vein, branch of bile duct, and

branch of hepatic artery) across the filtrating and metabolically active sinusoid parenchyma, and finally into a centrally located central vein. The central vein culminates into the hepatic vein, the outflow venous structure of the liver, which in turn flows into the inferior vena cava, as it approaches the right atrium of the heart. Normal liver parenchyma has regenerative capacity and can recover from most minor insults, such as a hepatitis B or a night of binge drinking. But when the liver is chronically overwhelmed, either with medicines/toxins or circulatory load, then the sinusoidal micro-architecture becomes distorted by accumulation of fibrous bands called septa, and by the formation of nodules. When the hepatic micro-architecture is distorted, the flow across the liver parenchyma is occluded and slowed, causing pressure to build in the portal vein, and accumulation of unprocessed toxins to build, further damaging the micro-architecture. Thus, when this cycle repeats itself, the liver can no longer function properly, including neutralizing medicines/toxins, creating a positive feedback loop of sorts that culminated into liver fibrosis and cirrhosis. It is this inadvertent positive feedback loop created by worsening liver disease that permits the progression from reversible mild liver disease to irreversible severe liver disease. In general, the liver has incredible regenerative capacity, as it is the only organ that can regenerate itself completely, but this regenerative capacity is lost after repeated toxic insult. Characterizing the point at which this reversible to irreversible transformation occurs is the focus of this project.

Normal liver function in the human body includes a whole spectrum of metabolic and absorptive functions. In doing so, the liver receives 25% percent of cardiac output, while weighing only 2.5% of the total body weight.

The liver circulation input is composed of the hepatic artery (off the parent celiac trunk of the aorta) and the portal vein (a vein joining outflow from the gastrointestinal system and spleen, the superior mesenteric vein, and splenic and inferior mesenteric veins; joining abdominal visceral venous outflow). The venous inflow of the portal vein into the liver is destined for processing of

consumed nutrients into molecules for physiologic use, and for processing of medications, toxins, and most ingested foreign substances. Arterial inflow from the hepatic artery into the liver provides the delivery of oxygen to the energy-demanding cells involved in the metabolic processing and detoxification of portal circulation.

Because the liver receives such a large percentage of cardiac output, its flow – and any change to it – has equally as large an impact on systemic circulation. When systemic circulation becomes altered, organs that heavily rely upon flow are also affected, such as the kidneys, heart, and brain. The liver, heart, and kidneys are closely linked to one another not only by physical circulation, but they are also linked by the renin-angiotensin and nervous system axes, which aid in modulating flow and perfusion within systemic vasculature. This is an important far-reaching impact of the liver because biomarkers and physical examination of the kidney, heart, and brain can aid in indirectly accessing the extent of liver disease.

Chronic toxic insult of the hepatic parenchyma by any toxin, such as alcohol, involves complex biochemical and pathophysiologic processes. In acute alcohol overuse, the toxic effects initially present as histologically detectable accumulation of fat molecules within the sinusoidal liver microarchitecture, pathologically called alcoholic steatosis. It is important to note that at this stage, the liver can still regenerate from this state. Indeed, a night of binge drinking may result in enlarged fatty livers, but a week of abstinence will result in return to baseline liver size. In chronic alcohol overuse, the toxic effects pass the point of regeneration and present histologically as fibrotic bands visible on a trichrome stain, and present clinically as portal hypertension. This is a state of *liver fibrosis*. These fibrotic bands prevent the normal flow of blood through the liver parenchyma and there is an accumulation of pressure resulting in portal hypertension.

Clinically, the measured pressure of the portal vein is called the portal pressure. A state of chronically elevated portal pressure is a state of portal hypertension (PH). In the clinical

management of a fibrotic liver, portal pressure, liver circulatory inflow pressure as compared to the hepatic vein pressure, liver circulatory outflow pressure, is serially measured. The gradient between pressures measured at the portal vein and hepatic vein is called the Hepatic Vein Pressure Gradient (HVPG). Normal HPVG is 1-5 mmHg, and anything 6 or greater is considered PH. Clinically Significant Portal Hypertension (CSPH), anything greater than or equal to 10mmHg, is the pressure gradient associated with clinical manifestations of PH, such as abdominal ascites, esophageal varices, or pleural effusions. These manifestations carry grave risk with them, as they can result in spontaneous bacterial peritonitis, gastric variceal hemorrhage, and respiratory distress secondary to pulmonary edema. Chronic hypertension left untreated progresses beyond severe liver disease and provides the molecular background for development of Hepatocellular Carcinoma (HCC).

Even in the absence of HCC, PH has severe effects on circulation and several metabolic processes. PH with end-stage liver disease should be thought of as manifesting in two main states: early and late. In early portal hypertension and liver disease, systolic blood pressure will be elevated, as the arterial pressure elevates to physiologically complement the elevated venous pressure from portal hypertension. In late chronic portal hypertension with end-stage liver disease, patients develop what is called *hepatorenal syndrome*, where the perturbation from portal hypertension of built up venous pressure results in progressive kidney failure. Eventually, PH leads to renal failure and right-sided heart failure.

As liver disease progresses and venous pressure builds, the venous outflow from the splanchnic visceral organs decreases and causes the decrease of systemic venous resistance, which thought to result from the release of splanchnic endothelial nitrous oxide. As venous resistance falls, there is a rise in cardiac output. This fall in venous systemic resistance causes a decrease in mean arterial pressure. As a result of this developing hepatorenal syndrome, it is thought that the release of systemic vasodilators aid in splanchnic circulation as outflow through liver slows and venous

pressure rises. Chronic buildup of venous pressure leads to hepatorenal syndrome, which further contributes to the accumulation of toxins in the blood, as the liver is ano longer able to metabolize toxins and the kidneys can no longer excrete them. The drop in systemic vascular resistance results in attempted compensation of the kidneys to increase pressure by release of anti-diuretic hormone (ADH), which in late end-stage liver disease become measureable. These pathophysiological relationships are important in understanding the measurable manifestations of liver disease and PH that are used in treating and assessing severity of liver disease in humans.

Liver Disease is a generic term used to describes disease pathology manifesting not only in the loss of hepatic function, but also in secondary effects due to the liver ceasing to perfuse and the resultant development of portal hypertension. In this study, the term *liver disease* refers to an intrahepatic liver disease state known as cirrhosis, a state of hepatic fibrosis physiologically most notably characterized by elevated liver enzymes and loss of essential protein, histologically characterized by the distortion of normal hepatic micro-architecture by fibrotic septa, and clinically characterized by systemic signs of portal hypertension, such as abdominal ascites, formation of collateral circulation, hepatic encephalopathy, esophageal varices, and pulmonary effusions. In the compensated cirrhosis state, the distorted micro-architecture of the liver can regenerate and return to normal histological structure and physiologic function with corrective lifestyle change and management of increased portal pressure. But in the decompensated cirrhosis state, the regenerative capacity of the liver is lost and these fibrotic bands accumulate to dominate the hepatic-microarchitecture with fibrosis and outflow obstruction. In any case of alcohol relate liver disease, inflammatory cell infiltration is more apparent than in non-alcoholic fatty liver disease(Toshikuni, Tsutsumi, and Arisawa 2014) (NAFLD).

When a patient is diagnosed with liver disease, a symptomatic presentation or history aids in diagnosing type of liver disease and assessing the extent liver disease. Patients will likely have

presented with milder signs of clinically relevant portal hypertension, such as spider nevi, gynecomastia, testicular atrophy, fetor hepaticus, asterixis, tendency to form ecchymosis, ankle edema, or scleral icterus, to more severe symptoms such as hepatic encephalopathy, anemia, tendency to bleed and measurable coagulopathy, esophageal or anal varices with or without hematemesis and/or melena, splenomegaly, caput medusae, ascites, or hypertensive gastropathy. Having a known history of chronic alcohol overuse will likely prompt monitoring for liver disease by a provider. The typical measures of liver disease include both directly-linked and indirectly-linked measures: vital signs, complete metabolic panel, complete blood count, coagulation profile, and liver function tests. The outcome of these measures combined with a past medical history will determine what kind of liver disease (i.e. alcohol liver disease versus fatty-liver disease).

Hypertension is typically associated with "high blood pressure," meaning systolic blood pressure is elevated. In the natural history of liver disease, a patient might first have hypertension, but may be normotensive or develop hypotension as their liver disease worsens progress to developing hepatorenal syndrome.

The complete metabolic panel is an incredibly useful clinical tool, and includes blood serum levels of sodium, potassium, chloride, bicarbonate, blood urea nitrogen (BUN), creatinine, and glucose. In advanced cirrhosis, patients may have hyponatremia or elevated creatinine. Hyponatremia occurs because of elevated ADH levels secondary to hepatorenal syndrome, which results in the cessation of water excretion in the kidneys. Creatinine levels rise as the severity of hepatorenal syndrome progresses.

A complete blood count (CBC) and differential includes white blood cell count (10^3 μL), red blood cell count (10^3 μL), hemoglobin concentration (g/dL), hematocrit percentage, mean corpuscular volume of red blood cells (femtoliters, fL), mean corpuscular hemoglobin (pg), mean cell hemoglobin concentration (g/dL), red blood cell distribution width percentage, platelet count

(10^3 μL), and percentage of lymphocytes, monocytes, neutrophils, eosinophils, and basophils. The main changes of the CBC and differential seen in PH are cytopenia (low platelets), anemia, and leukopenia (low white blood cells).

In PH, because portal flow combines splanchnic and splenic outflow, splenic congestion results in up to 90% platelet sequestration and splenomegaly. Cytopenia from this etiology tends to result in platelet counts less than 50,000/mL. Splenic congestion may also result in leukopenia, due to sequestration of white blood cells, and neutropenia, due to sequestration of neutrophils.

Anemia, or low hemoglobin, when present with liver disease results from multiple pathophysiologic processes. Hemoglobin loss may be due to gastrointestinal bleeding , folate deficiency, or directly due to effects of toxic effects of alcohol, bone marrow suppression, anemia of chronic disease, splenic sequestration, or progressive renal failure.

The liver plays an immense role in systemic ability to coagulate. Thrombopoietin produced in the liver regulate platelet production in the bone marrow. The liver produces both coagulation factors, I, II, V, VII-XII, and anticoagulation factors, protein C, protein S, and antithrombin(factor III), and even modulators of fibrinolysis, plasminogen and antiplasmin. Without these factors, both the intrinsic and extrinsic clotting cascades are unable to function properly, and systemic circulation is both prone to bleeding but unable to stop clot propagation once it begins. In liver disease, prothrombin time (PT), a measure of extrinsic clotting cascade function, and partial thromboplastin time (PTT), a measure of intrinsic clotting cascade function, are both elevated. International normalized ratio (INR) is a ratio of the patient's PT and an internationally accepted PT; an INR of 1.0 indicates a "normal" INR and >1.0 indicates a dysfunction of normal coagulation pathways. Targeted anticoagulation therapy often aims for an INR of 2.0-3.0, and INR >3.0 is often considered inoperable.

Serum levels of aspartate aminotransferase (AST) and alanine aminotransferase (ALT) are enzymes involved in amino acid metabolism by the liver. AST is found in the liver, skeletal muscle, kidneys, brain, heart, and red blood cells. ALT is also found in red blood cells, but mainly in the liver. Both AST and ALT are elevated in liver disease and considered *the* biomarkers of liver disease. In early and moderate alcohol cirrhotic liver disease, AST is usually more elevated in ALT, in approximately a 2:1 ratio. In late alcohol cirrhotic liver disease, AST and ALT may not be elevated because liver parenchyma is no longer functional enough to release enough AST and ALT to be elevated; both are often normal.

Alkaline phosphatase is a dephosphorylating enzyme that is found in skeletal and liver tissue. Alkaline phosphatase levels are usually elevated in cirrhosis, but not more than three times the upper normal limit which could indicate another etiology. Degree of elevation is an important distinction to differentiate primary liver disease versus biliary disease.

Gamma-glutamyl transpeptidase (GGT) is an important enzyme involved in regeneration of glutathione and detoxification of physiologic toxins, a main function of the liver. GGT levels tends to be proportional with alkaline phosphatase levels in liver disease but are non-specific. GGT elevation is more prominent in alcohol liver disease than in other etiologies of liver disease.

Bilirubin is a normally produced compound from red blood cell catabolism as they are recycled every 120 days. Bilirubin is then excreted in bile during digestion of fats, urine (as urobilin), and stool (as stercobilin). Bile is formed in the liver sinusoidal parenchyma and flows towards the confluence of bile cuniculi to form the hepatic duct and into the gallbladder where bile is stored. When liver fibrosis causes flow congestion in the liver parenchyma, bile flow congests as well, and total serum bilirubin levels rise.

Albumin is a key serum protein produced in the liver that binds water, fatty acids, hormones, bilirubin, cations, and other compounds. As liver fibrosis and subsequent cirrhosis progresses,

albumin production will fall. Therefore, when there is known liver disease, serum albumin levels are a direct indication of liver disease severity. However, serum levels of globulins are commonly elevated in cirrhotic patients. It is thought that this is due to the shunting of venous blood away from the liver directly to lymphoid tissue, where a more acute reaction results in immunoglobulin production.

ii. Relevant Epidemiology

This section will include relevant population-level epidemiology of liver disease, including that of cirrhosis and hepatocellular carcinoma.

In humans, cirrhosis develops over a long period of chronic alcohol abuse or chronic accumulation of fat molecules in the liver, due to diet, genetics, or drug side-effects; either Alcohol Liver Disease (ALD) or Non-alcoholic fatty liver disease (NAFLD). A fibrotic and cirrhotic liver, from either etiology, provides the molecular background for the development of hepatocellular carcinoma (HCC). However, it is not known worldwide what percentage of liver disease can be attributed to alcohol use(Toshikuni, Tsutsumi, and Arisawa 2014). This is largely due to the varying rates of alcohol consumption in different parts of the world.

The threshold for developing alcohol cirrhosis is about 80 g/day for 10-20 years(Sofair et al. 2010) but fibrosis, or clinical liver cirrhosis, can occur with lower doses of alcohol in some populations. Of those patients with alcoholic steatosis, one-third will develop fibrosis and 10% will develop alcoholic cirrhosis(Kim and Han 2012). Of those with alcoholic cirrhosis, 1-2% will develop HCC. Alcohol consumption, of either 50 g/day or 100 g/day, increases the relative risk of HCC to 1.36 and 1.86, respectively. It is unknown what causal effects alcohol, in any amount, may have on a liver already affected by a Hepatitis B or C viral infection. Overall, there is a clear link of alcohol with liver fibrosis and cirrhosis, and subsequent development of HCC. However, there is no

definitive management plan tailored to the molecular changes related to alcoholic cirrhosis or to the amelioration of portal hypertension and associated symptomatology.

Worldwide, liver disease causes an estimated one million deaths worldwide annually. Alcohol Liver Disease alone causes 500 million of those deaths, annually, even though it is not the major cause of liver disease worldwide. Among newly diagnosed cases of liver disease, the profile of an average ALD patient is an American white male, aged 45 or greater, graduated from high school with or without college, of variable employment status, with an annual income of less than $47,000/year, most likely with managed care health insurance, with 91.5% having a history of heavy drinking for more than 20 years(Sofair et al. 2010). ALD is a condition that afflicts a major sector of the U.S. population – males comprise about 31% of the U.S. population alone, with overall fatality rates of alcohol-related liver disease approaching 7 per 100,000 annually(Yang 2008). And indeed, it has been shown that women have more severe liver damage with the same dosage of alcohol consumption as compared to men(Toshikuni, Tsutsumi, and Arisawa 2014; Sofair et al. 2010). A meta-analysis pooled relative risk of men and women with alcohol liver disease of developing liver cancer and found that with heavy drinking, men had a 1.59 relative risk of developing HCC and women had a 3.89 relative risk of developing HCC(Bagnardi et al. 2015). Therefore, at the same level of alcohol consumption, women experience higher rates of worsening ALD.

ALD results in more deaths annually in proportion to the amount of newly diagnosed liver disease caused by alcohol use, with over a third of the U.S. population more at risk for having a diagnosis of alcohol liver disease(Rowe 2017). Annually, about 1.0-3.1% of patients with simple hepatic steatosis progress to liver cirrhosis, and 3.2-12.2% of patients with steatohepatitis progress to liver cirrhosis(Toshikuni, Tsutsumi, and Arisawa 2014).

Alcohol related disease, including HCC, contributes 4.6% of disability-adjusted life-years and 3.8% of all deaths(Rehm et al. 2009). In a study of decompensated alcohol cirrhotic patients, those

with older age were more likely to have HCC(Toshikuni, Tsutsumi, and Arisawa 2014). Overall cumulative incidence of HCC was 6.8% in patients with compensated ALD for 10 years and 7.1% in patients with decompensated ALD for 5 years(Sola et al. 2006). Importantly, approximately 88.0-94.7% of HCC arises from alcohol-related cirrhosis, much higher than HCC from NAFLD(Hashimoto, Taniai, and Tokushige 2013).

Additionally, the earlier the detection of HCC, the better the patient outcome(Kim and Han 2012). In patients with already-detected alcoholic liver cirrhosis, cause of mortality was HCC in 12.5-13.0%(Alvarez et al. 2011). Indeed, ALD is the largest contributor to liver disease mortality in the United States with 37% of deaths in 1998 attributable to ALD(Sofair et al. 2010). Therefore, the incidence of alcohol liver fibrosis/cirrhosis and the frequency with which it progresses to HCC indicates a need for an comprehensive animal model that captures a large portion of the liver fibrosis/cirrhosis to HCC continuum.

iii. Use of Oncopig Model in a Swine Model of Liver Fibrosis

The transgenic Oncopig Model (OCM) is a unique genotypically, anatomically, and physiologically relevant large animal model for preclinical study of human disease that develops site/cell specific tumors after Cre recombinase exposure(Schook et al. 2015). The OCM was designed to harbor mutations found in more than 50% of human cancers: KRASG12D and TP53R167H, which commonly occur in HCC(Lee 2015) and result in a OCM HCC that recapitulates the phenotype and physiology of human tumors(Schachtschneider et al. 2017).

The OCM effectively addresses relevant murine model deficiencies. In the OCM, TERT is silenced in OCM somatic cells and is solely expressed in OCM cancer cells(Schachtschneider et al. 2017), and innate OCM KRASG12D and TP53R167H germline mutations are heterozygous in nature, closely modeling human disease(Schook et al. 2015). Because HCC does not develop from a native pathology-free state, but rather after chronic toxic liver insult followed by compensatory

inflammatory and remodeling processes, the progression from liver fibrosis to liver cirrhosis in the OCM is key in creating an ideal and clinically analogous background for a model of HCC. The OCM thus represents a vital translational research technology for molecular characterization of oncogenesis that serves as a critical bridge between preclinical murine studies and human clinical practice and management of neoplasms.

As HCC develops in patients with liver fibrosis and cirrhosis, an ideal HCC model must also be able to reflect this comorbidity, and a method for monitoring clinical sequalae leading up to HCC. The ability to concurrently induce liver cirrhosis and HCC in the OCM through an analogous liver insult provides an efficient and relevant opportunity to assess the role of chronic liver disease in HCC tumorigenesis. While autochthonous HCC tumors have been developed in chemically induced porcine HCC models(Li et al. 2006; Mitchell et al. 2017), such models take over 1 year to develop clinically relevant tumors and do not allow for control of tumor number, location, or comorbidities. Thus, this makes these models less favorable for preclinical and co-clinical trials. The OCM addresses these weakness and does so through a molecularly analogous method to chronic liver disease, while capturing an epidemiologically relevant portion of the liver disease with progression to HCC continuum.

b. Related Literature

The section will summarize the background on other important features of this study, such as the economic burden of disease and animal models of liver disease.

i. Social Cost of Liver Disease

Liver disease is one of the top 20 causes of death in both developing and developed countries. In the United States, 1 in 10 adults suffers from liver disease with over 100 causes of liver disease, including ALD and NAFLD. In one study, the monetary social cost of heavy drinking was reported to be 1% or more of the gross domestic product in high-income countries(Mohapatra et al.

2010). The cost directly associated with managing and treating ALD throughout its course is not known. But importantly, approximately 88.0% to about 95% of Hepatocellular carcinoma (HCC) arises from alcohol-related cirrhosis, much higher than HCC from NAFLD(Hashimoto, Taniai, and Tokushige 2013). Because liver disease progresses to HCC, an expensive disease to treat with healthcare and social cost totaling to 1.6% of US GDP(Mohapatra et al. 2010), it is of interest to create a model that encompasses both a relevant portion of the liver disease continuum and capture the threshold at which ALD progresses to HCC.

ii. Liver Disease Models

When assessing the utility of an animal model of disease, it is necessary to evaluate the reproducibility of the disease, the specificity of the method, the cost of producing the model of disease, safety of the method, and the ethical considerations of the model. The majority of animal models of fibrosis and liver disease utilize small animal models, or do not utilize an etiologically analogous method to induce cirrhosis/fibrosis.

A large animal model of fibrosis, precursor to hepatocellular carcinoma, with a similar disease progression as seen in humans with validated laboratory values and histology markers would provide an avenue for developing and testing new minimally invasive local therapies for liver fibrosis and cirrhosis and hepatocellular carcinoma.

Animal models of fibrosis either use an anatomical method to restrict portal flow acutely, or chemical methods to restrict portal flow in a delayed or chronic fashion(Geerts et al. 2008). Animal models altering pre-hepatic or intra-hepatic flow utilize Poiseuille's equation of blood flow to induce portal hypertension and theoretically subsequent liver fibrosis/cirrhosis.

Partial portal vein ligation has been developed as a method to produced calibrated stenosis of the portal vein in rats, mice, and rabbits. Maximal portal hypertension through vein ligation is

achieved at 24 hours, while experimental infection with schistosoma mansonia in mice and hamsters produced portal hypertension as early as 7 weeks(Abraldes, Pasarin, and Garcia-Pagan 2006).

Structural models of portal hypertension induce measurable portal hypertension fast enough to have research utility but have not proven to produce sustained portal hypertension or clinical relevant liver disease, especially not in a manner that is pathophysiologically analogous to human liver disease.

Bile duct ligation for induction of chronic cholestasis is able to induce liver inflammation and areas of liver necrosis with accompanying elevations in AST and ALT, but does not induce histologically evident liver fibrosis (Dondorf et al. 2017).

Chemical methods of hepatic injury have also been shown to induce portal hypertension and liver cirrhosis(Abraldes, Pasarin, and Garcia-Pagan 2006; Bosch and Iwakiri 2017). This includes the use of carbon tetrachloride (CCl_4), thioacetamide (TAA), dimethylnitrosamine (DMNA)(Ding et al. 2017), and diethylnitrosamine (DEN)(Mercer, Hennings, and Ronis 2015) in inducing similar inflammatory and biochemical processes that are relevant for HCC. Some models use a combination of these hepatic toxins to increase incidence of hepatocellular carcinoma(Xin et al. 2017). However, these models have not been validated via histology, serum biomarkers, or clinical assessment, and are not pathophysiologically relevant to liver disease with progression to HCC.

Additionally, diet-induced cirrhosis has also been shown to induce fibrosis and cirrhosis(Santhekadur, Kumar, and Sanyal 2017), and is certainly a clinical relevant model as animal models fed a generally high fat diet, diet high in high-fructose corn syrup, choline-deficient L-amino acid diet (CDAA)(Ikawa-Yoshida et al. 2017), or a diet generally high in cholesterol have all been shown to induce non-alcoholic fatty liver disease (NAFLD), or also known as non-alcoholic steatohepatitis (NASH)(Wu 2016). A diet high in fat is a major risk factor, but these have not been

well hemodynamically characterized, and are less cost effective due to the time frame that clinically relevant liver fibrosis, cirrhosis, and HCC develop.

There is also potential for discussion of safety and ethical considerations when an experimental model requires the inoculation of an animal with a known parasite or known carcinogen, or the force feeding of a high-fat diet.

In a mice model of HCC using DEN, a known inducer of HCC, when ethanol was added, the liver tissue was shown to have increased activation of inflammatory pathways and HCC-relevant pathways in non-tumor hepatic tissue(Mercer, Hennings, and Ronis 2015; Ambade et al. 2016). Ethanol is a clinically relevant hepatic toxin, with heavy alcohol consumption being a primary risk factor in up to one-third of HCC cases(Hassan et al. 2002), and is a cost-effective method to induce liver fibrosis due to its acute development and potential for persistent fibrosis. Hepatocyte exposure to ethanol induces the activation of biomolecular pathways relevant for HCC(L. Wang et al. 2017). It has been shown that a comparable swine model for portal hypertension utilizing a weight-based dose of ethiodized oil:ethanol mixture model may induce liver fibrosis, according to METAVIR score, at 2-weeks and can persist for up to 6 weeks (Avritscher et al. 2011). However, there has not yet been a swine model of liver fibrosis, which leads to liver fibrosis and that has shown persistent fibrosis at 8 weeks or beyond. Further, it is unknown how long these effects persist, which is relevant for long-term studies of interventional management and oncological treatment. Animal models of portal hypertension and liver fibrosis are summarized in Table I.

c. Purpose of Study

The purpose of this study is to create a large animal model of alcohol liver fibrosis using the swine OCM. This project is a proof-of-concept study for a research model that reproduces the clinical course of alcoholic cirrhosis as seen in humans through the comparison of clinical presentation, serial serum laboratory biomarker values, and liver histopathology. This study will aid

in standardizing a large animal model of liver fibrosis so that medical and interventional treatment studies may more efficiently and reliably transition from animal model to clinical trial when studying liver fibrosis with progression to HCC.

d. Significance of Study

Liver disease affects 10% of the world's population and is one of the top 20 causes of death in developing countries(Rowe 2017). This study will be integral in elucidating the molecular and pathophysiological changes that underlie chronic alcohol liver injury resulting in alcoholic liver fibrosis. By providing a clinically comparative model through the use of symptomatology, histology, and serum laboratory biomarker values, this study will also provide the comparative basis for the use of a large animal model in predicting performance of both medical management and procedural intervention research in human clinical trials.

TABLE I SUMMARY TABLE OF ANIMAL MODELS OF PORTAL HYPERTENSION AND LIVER FIBROSIS

Model	Type	Size	Pro	Con	Group
Portal Vein Ligation	Anatomical	small	PH at 24 hrs	Effect not sustained	Geerts et al 2008
Schistosoma mansonia infxn	Anatomical	small	PH within 7 wks	Effect not sustained	Abraldes et al 2006
Bile Duct Ligation	Anatomical	small	↑ LFTs	No fibrosis	Dondorf et al 2017
CCl_4	Chemical	small	PH and Hepatic Injury	Not validated Not analogous	Bosch et al 2017
thioacetamide (TAA)	Chemical	small	PH and Hepatic Injury	Not validated Not analogous	Bosch et al 2017
dimethylnitrosamine (DMNA)	Chemical	small	PH and Hepatic Injury	Not validated Not analogous	Ding et al 2017
diethylnitrosamine (DEN)	Chemical	small	PH and Hepatic Injury	Not validated Not analogous	Mercer et al 2015 Ambade et al 2016
Combination	Chemical	small	PH and Hepatic Injury	Not validated Not analogous	Xin et al 2017
Choline-Deficient L-Amino Acid Diet	Diet	small	Analogous	Time and money cost	Ikawa-Yoshida et al 2017 Wu et al 2016
Fibrosis Induction Procedure	Chemical/ Anatomical	large	Fibrosis at 2 weeks, up to 6 weeks	Not shown to persist to 8-weeks or more	Avritscher et al 2011

II. RESEARCH QUESTION

The main research question that this study aims to answer is: Is there an easily reproducible and clinically relevant animal model of alcohol liver fibrosis? That is, the aim of this study is to create a large animal model that correlates clinically with the natural course of alcohol liver fibrosis/cirrhosis as seen in humans. This model will be utilized both as a model to investigate the creation and outcome of surgical intervention in patients with liver fibrosis, and will also serve as a molecular background for the development of common gastrointestinal neoplasms, with HCC being the most directly relevant to alcohol liver disease.

a. Approach to Research Question

The approach to the research question utilized a practical methodology with the aim to induce liver fibrosis. The aim was to cause ethanol-induced hepatic inflammation and damage with the end goal being liver fibrosis. Liver fibrosis results from cyclical damage-repair cycles of hepatocyte inflammation and subsequent regeneration into fibrous bands that alter the hepatic parenchyma and normal liver flow. Therefore, the main strategy in addressing the research question was to induce hepatic damage locally to the liver parenchyma by administering a dosage of ethanol:ethiodized oil emulsion through the hepatic artery. If there was enough toxic damage to hepatocytes, then an increase in inflammation and fibrosis results in histologically apparent liver fibrosis.

b. Conceptual Framework

The conceptual framework of the research design for liver fibrosis induction progresses across three basic stages: fibrosis induction, serial monitoring of swine subject, euthanasia and necropsy at conclusion. This project is designed to utilize human-analogous timepoints and metrics for disease monitoring following ethanol toxic insult, as is achieved by the fibrosis induction procedure. Figure 1 illustrates this conceptual framework for this swine model of fibrosis induction.

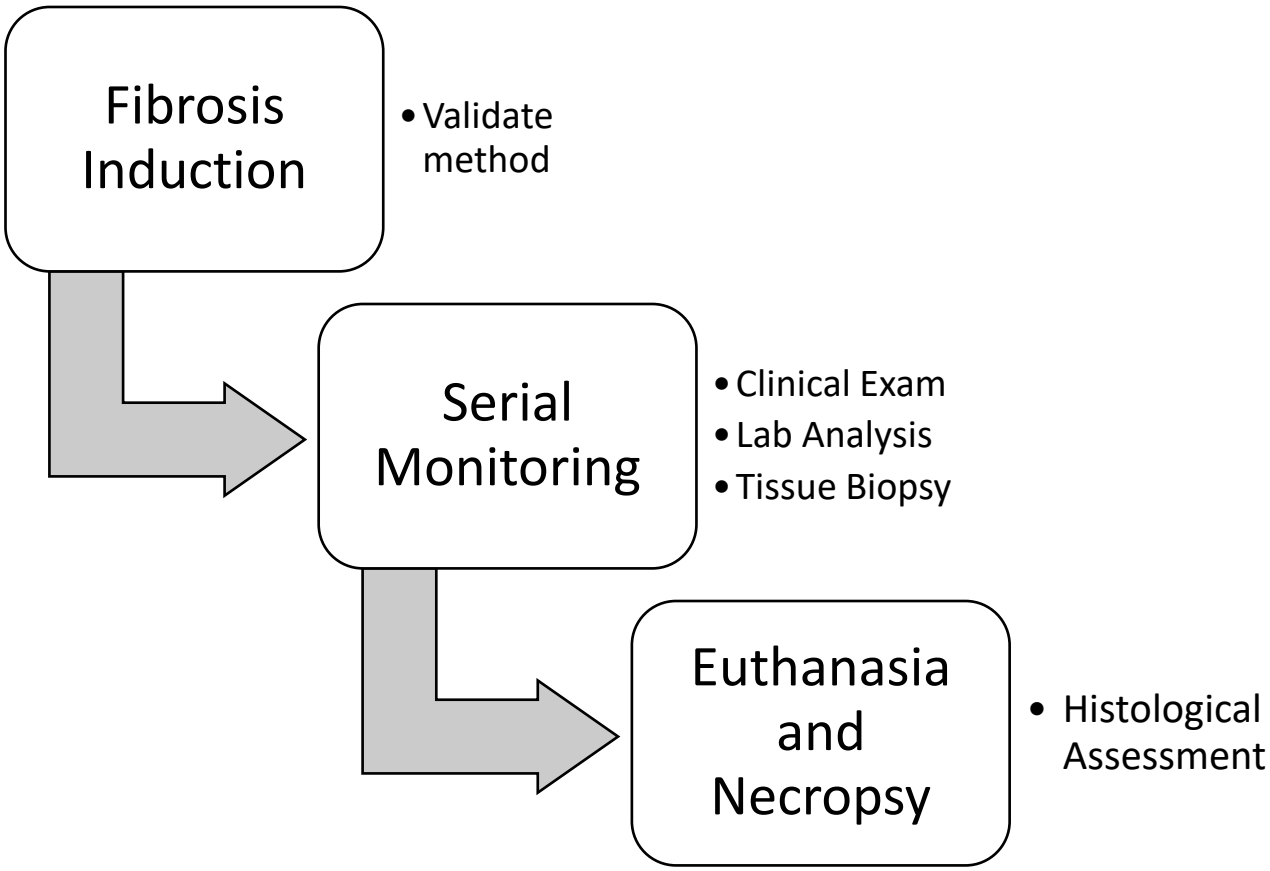

Figure 1 Conceptual framework for a swine model of fibrosis induction.

III. METHODS

Work was completed at the University of Illinois at Chicago and the University of Illinois at Urbana-Champagne. Both institutions are fully accredited by the Association for Assessment and Accreditation of Laboratory Animal Care (AAALAC) International. Institutional Animal Care and Use Committee (IACUC) approval was obtained before any procedures were initiated.

a. Study Design

This study utilized two experimental cohorts undergoing fibrosis induction done by a minimally invasive procedure. This is done by introducing a microcatheter through the femoral artery to directly inject a weight-based dose of lipdiol:ethanol emulsified solution directly into arterial liver circulation. A lipiodol:ethanol emulsion in a 3:1 ratio was utilized in the infusion procedure because the lipiodol component slows flow to maximize surface contact of the ethanol with surrounding structures(Madoff et al. 2007), and the contrast component of the lipiodol provides a real-time method to view infusion of ethanol, while the ethanol provides the toxic insult to the surrounding liver parenchyma.

The goal of the minimally invasive fibrosis induction procedure is to deliver a toxic dose of the lipiodol:ethanol emulsion at the beginning of hepatic arterial flow so that downstream flow will facilitate global hepatic infiltration with the lipiodol:ethanol emulsion and thus global toxic insults eventually resulting in fibrotic remodeling of liver parenchyma. Through femoral arterial access using ultrasound guidance, a microcatheter is utilized to locally deliver the ethiodized emulsion at the hepatic artery, before bifurcation into right and left branches corresponding to the right and left lobes of the liver (Figure 2).

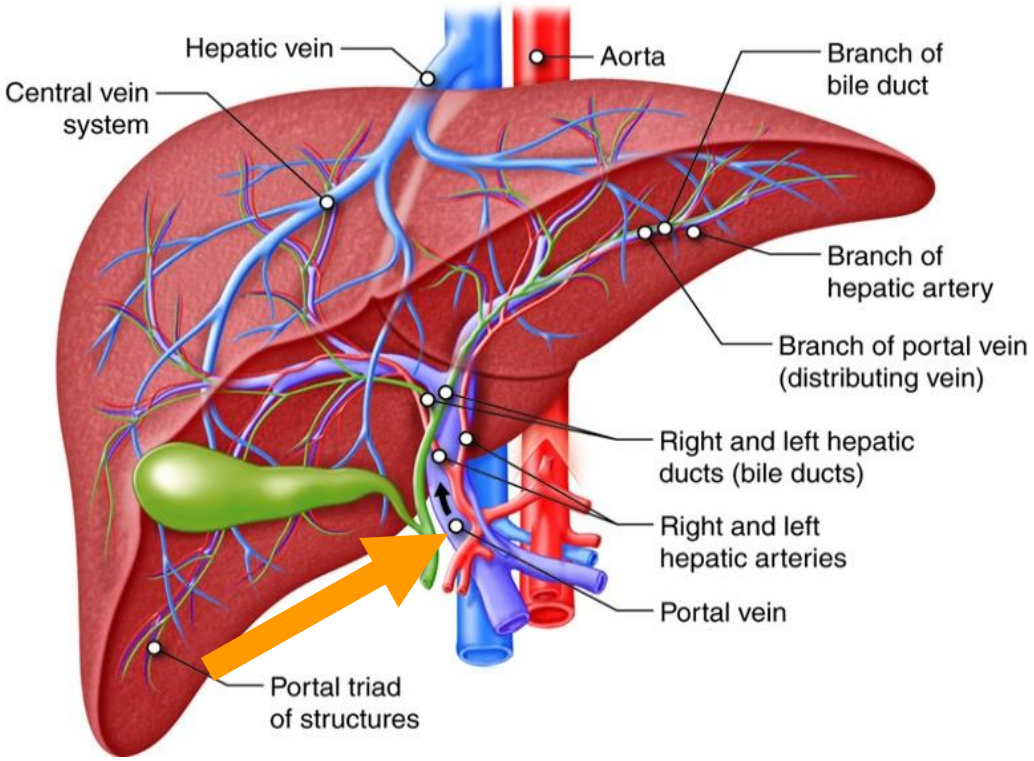

Figure 2 Anatomic diagram of hepatic circulation, including hepatic arteries and branching. Orange arrow indicates ideal location for lipiodol:ethanol emulsion delivery.

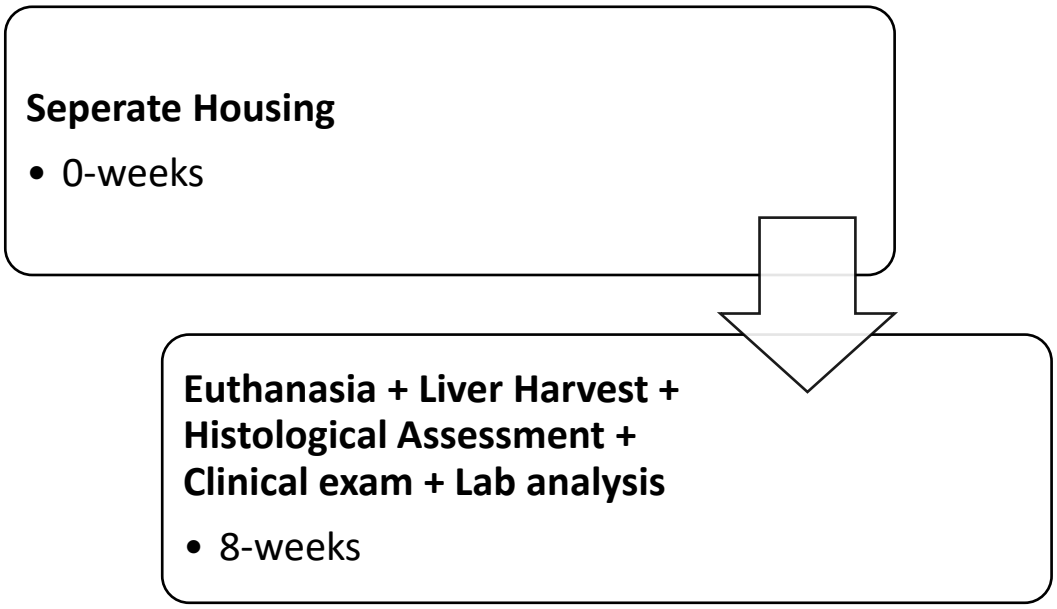

Figure 3 Control Cohort: Time Course for Comparison of Disease Course.

The study design utilizes 3 total cohorts, 2 experimental cohorts and 1 control cohort. The experimental cohorts were done separately in 2 cohorts so that they could be sequentially staged. In experimental cohort 1, the fibrosis induction procedure was performed at 0-weeks, bi-weekly laboratory values collected from 4-weeks through 6-weeks, and final necropsy of liver was performed at 8-weeks. In experimental cohort 2, the fibrosis induction procedure was performed at 0-weeks, serial biopsies are taken every two weeks for a total of 8 weeks post-induction, and final necropsy for liver tissue was done at 20-weeks. For both experimental cohort 1 and 2, bi-weekly clinical exam and lab values are collected and compared at 0-, 2-, 4-, 6-, and 8-weeks. All liver biopsies taken at 4-weeks, 6-weeks, and 8-weeks were evaluated for histopathologic features that signal developing fibrosis and inflammation in the liver tissue, utilizing trichrome and hematoxylin and eosin stain. For both cohorts, histological analysis of fibrotic liver was compared to normal-appearing liver from both the external control group of age- and gender-matched healthy controls, and a pseudo-internal control group utilizing normal-appearing liver tissue from experimental cohort samples. All animal procedures were performed according to the experimental protocol approved by IACUC.

b. Timeline

The control cohort (n=5) was separated from their weening litter at 0-weeks. At 8-weeks, weight and serum laboratories were collected for comparison across both experimental groups at the same timepoint. Necropsy was performed for comparison to healthy age- and gender-matched controls (Fig 3).

In the first experiment, the aim was to validate the success of a previously published protocol(Avritscher et al. 2011) to produce liver fibrosis in the OCM. Therefore, in the OCM cohort 1 (n = 5), liver injury was induced and followed by post-induction disease surveillance via bi-weekly lab analysis, with subsequent euthanasia, liver harvest, and liver histological assessment at 8-weeks

post-induction (Fig. 4). Laboratory and histological results were also compared to age- and gender-matched healthy controls (n = 5). Following validation of fibrosis induction in Oncopigs, the procedure was repeated for an extended time course experiment in OCM cohort 2 (n = 5) to investigate disease progression and the capacity of the fibrosis induction procedure to provoke sustained liver disease. In this second OCM cohort, physical examination, lab analysis, and serial liver biopsies were obtained at 2-week intervals for a total of 20-weeks, followed by euthanasia, liver harvest, and histological assessment (Fig. 5).

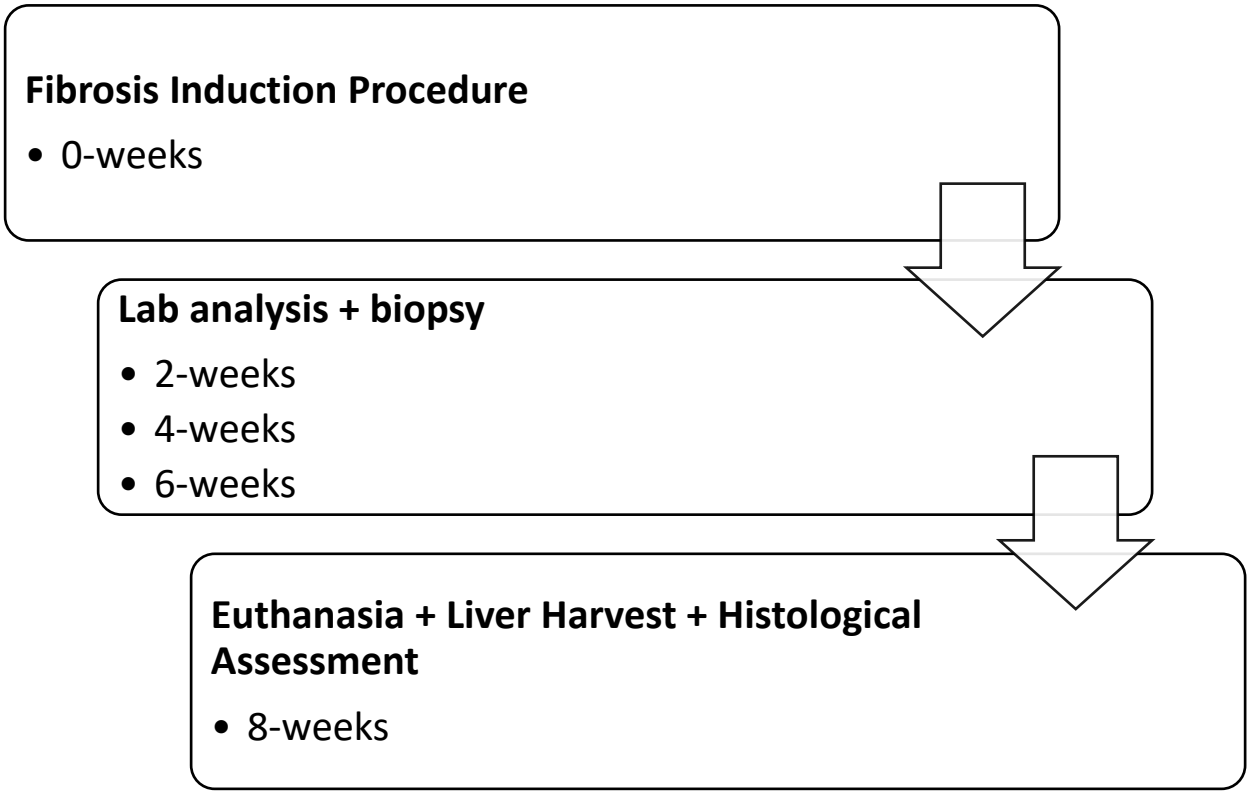

Figure 4 Cohort 1: Validation of Fibrosis Induction Time Course.

i. Animal Care

Animals were housed in the Biological Research Laboratory at each respective site – University of Illinois in Urbana-Champaign for cohort 1 and University of Illinois at Chicago for cohort 2 – and monitored daily by an on-site veterinarian (K.D.G.) with 20 years of experience. Daily examination included observation of behavior and eating habits, as well as any neurological abnormalities.

ii. Serum Laboratory Collection

Baseline porcine serum laboratory normal ranges are generally unknown for piglets, as they fluctuate from weaning through adolescence onto adulthood, and also in the OCM used in this study. Therefore, any statistically significant findings were done comparing to an age-matched

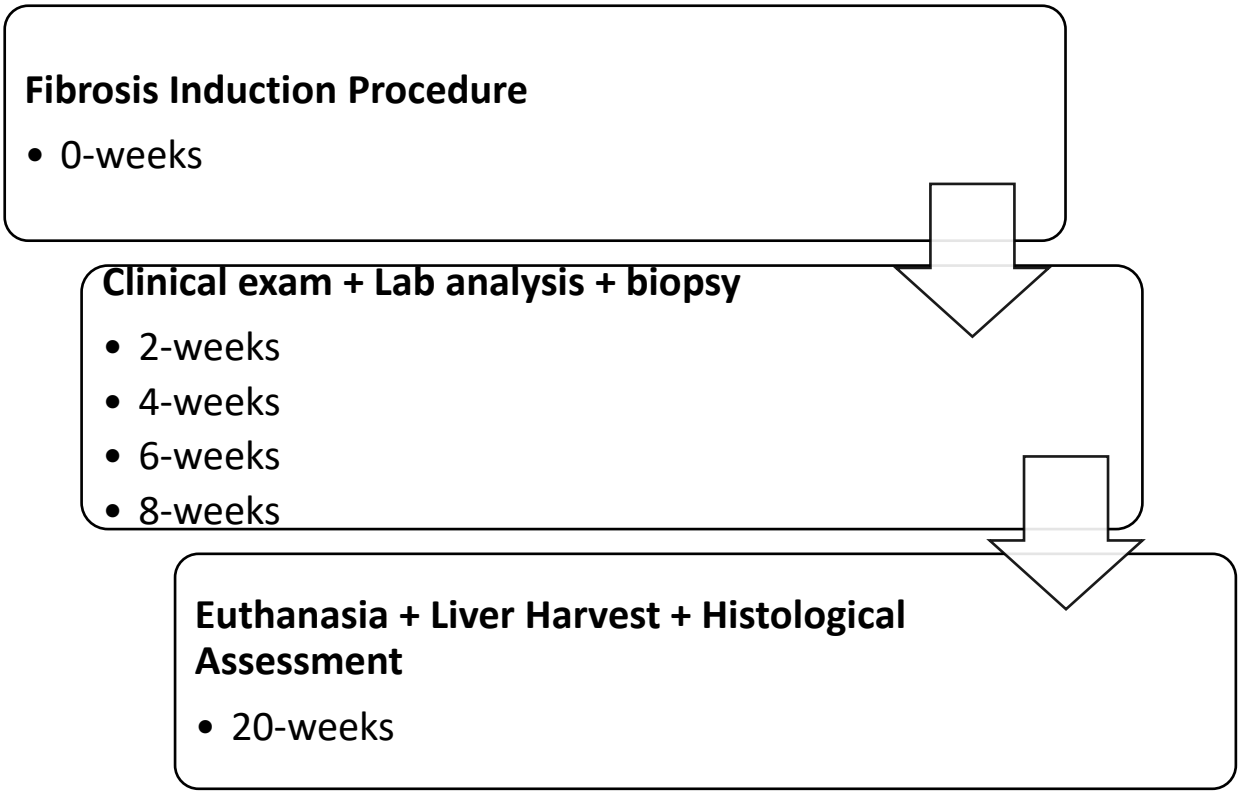

Figure 5 Cohort 2: Extended Time Course for Study of Disease Course.

control group housed in the same facility as the experimental subjects. There was no difference in diet, observation, or exercise between the experimental cohorts and control cohorts that were housed in the same facility with the same feeding and sleep schedule.

Serum laboratories for cohort 1 were collected on the day of the induction procedure for a baseline level, 0-weeks, and serially at 4-weeks, 6-weeks, and finally, at necropsy at 8-weeks. Serum laboratories for cohort 2 were collected on the day of the induction procedure for a baseline level, 0-weeks, and serially bi-weekly until 8-weeks, and finally at necropsy at 20-weeks.

There may be some variability in serum laboratories due to the use of different laboratories to process serum samples and due to inherent differences across animal facilities in housing the two experimental cohorts and control cohort.

iii. Clinical Assessment

Daily animal care was supervised and monitored by veterinarian and veterinarian technicians. An overall observational assessment was done at 0-weeks to learn baseline behavior and energy level of piglets, and to confirm it was within the normal range of behavior. Daily clinical evaluation assessed general appearance and activity, along with appetite, a huge indicator of health in the swine species.

After induction and all biopsy procedures, ultrasound and neurological assessment was done to evaluate the effect of induction and biopsy procedures, as well as daily to evaluate for the possibility of hepatic encephalopathy due to the toxic effects on the liver of the lipiodol:ethanol emulsion infusion. Assessment also included behavioral assessment of general appearance (quiet vs. "bright, alert, and responsive), cooperativity, and appropriate body condition, and appetite.

Oncopig model subjects in cohort 2 underwent clinical assessment at baseline and biweekly post-induction thereafter, which included evaluation for the presence of ascites via ultrasound

examination, as well as examination for the presence of hepatic encephalopathy (HE) resulting in neurologic impairment.

Neurological assessment was done performing a "crossed-leg" placement test in which one hind leg of the pig is crossed over the other at one time(Jackson and Cockcroft 2002). Normal result is when a pig immediately uncrosses their legs without difficulty, while an abnormal response in impaired subjects may be a delayed reaction or inability to uncross their legs. This assessment also included gait assessment for instability or ataxia.

Neurological assessment was initially done utilizing an established neurologic deficit scoring system for swine models, traditionally used in resuscitation studies(Forbess et al. 1995; Allen et al. 2003). However, when no neurological deficit was noticed and all subjects in all cohorts received a score of 0 indicating "normal" neurological function, this scoring system was not utilized further.

c. Fibrosis Induction Procedure

All fibrosis induction procedures were performed by one of two board-certified Interventional Radiology (IR) physicians with 9 years (R.C.G.) and 4 years (R.P.L.) of clinical attending experience, according to a modification of the methodology described by Avritscher et al(Avritscher et al. 2011).

At 8-weeks of age, Oncopigs underwent anesthetic induction, followed by intubation and maintenance with 1-3% isoflurane. Angiography was performed using a C-arm (OEC Medical Systems series 9600; GE Healthcare, United Kingdom). With the animal in a supine position, the groin area was sterilely prepped and draped. Ultrasound-guided vascular access was gained via the common femoral artery with placement of a 5 French sheath (Pinnacle; Terumo Medical Corporation, Somerset NJ). Using standard catheter and wire techniques, celiac arteriography was performed using a 5 French catheter (Sos Omni Selective; AngioDynamics, Latham NY) (Figure 6). A coaxial 3 French microcatheter (Renegade Hi-flo; Boston Scientific, Marlborough MA) was

advanced into the common hepatic artery. Common hepatic arteriography was performed using injection of iohexol (Omnipaque-300; Amersham Health, Princeton NJ). The microcatheter was then advanced into the proper hepatic artery, and 0.75 mL/kg of a 1:3 v/v emulsified mixture of absolute ethanol and ethiodized oil (Lipiodol; Guerbet, Villepinte France) was slowly infused via the microcatheter into the hepatic arterial circulation over a period of 30 minutes (Figure 7, 8). Dosing of the administered ethanol and ethiodized oil emulsion, 0.75 mL/kg, was derived by dividing the maximally tolerated dose by mean pig weight reported in the study of Avritscher et al(Avritscher et al. 2011). Upon completion of the ethanol and ethiodized oil injection, all devices were removed, and hemostasis was achieved via manual compression at the vascular access site and at least 90 minutes of limb immobilization. The same devices and procedure utilized in the performance of human liver arteriography were used in this study in order to maximize the translational impact. After induction procedures, animals were recovered, returned to their pens, and followed-up daily until sacrifice (cohort 1) or biopsy (cohort 2).

d. Biopsy Procedure

Percutaneous ultrasound-guided liver biopsy procedures were performed by a board-certified IR physician with 9 years of clinical attending experience (R.C.G.) or a medical student research associate (N.M.E.) under the direct supervision of one of three experienced practitioners, including a board-certified laboratory animal veterinarian with 20 years of clinical experience (K.D.G.), and a veterinarian with 2 years of experience in lab animal medicine (M.E.). Liver biopsies were undertaken in a surgical suite following animal subject intubation and maintenance under general anesthesia, as previously described. With the animal in a supine position, the abdomen was sterilely prepped and draped. Using ultrasound guidance, an 18-gauge automated biopsy device (BioPince; Argon Medical Devices, Plano TX) was advanced into the right liver lobe, and a 2-cm in length core specimen was attained; this was done a total of 3-4 times, sequentially obtained. The tissue cores

were transferred to a container with 10% neutral buffered formalin for fixation; the same sterile formalin containers used for human tissue biopsy processing. After liver biopsy, animals were recovered, returned to their pens, and monitored until sedation wore off and they returned to their baseline behavior. They were clinically followed-up daily until subsequent biopsy or sacrifice.

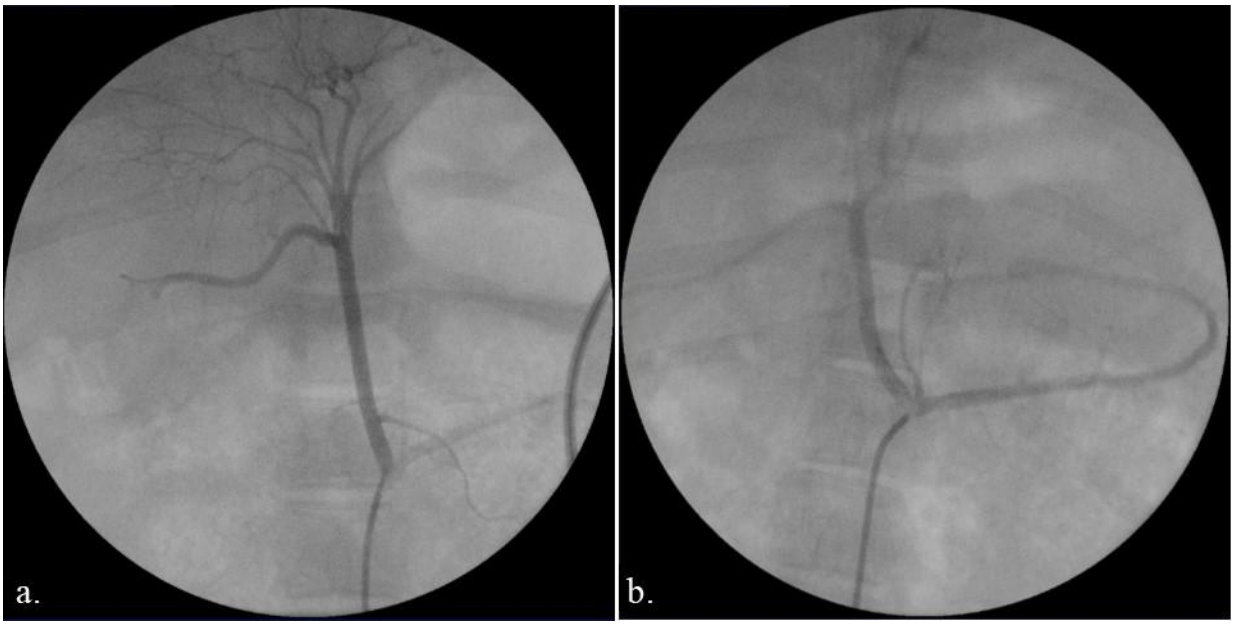

Figure 6 Representative images from fibrosis induction procedure (fluoroscopic images) of hepatic arterial circulation. (a) celiac arteriogram shows conventional porcine hepatic arteries before induction of PG 5601. (b) conventional porcine hepatic arteries before induction in PG 5603.

i. Laboratory Values

In the experimental cohorts 1+2, vital signs, complete metabolic panel, complete blood chemistry and differential, coagulation profile, and liver function tests were acquired the day of the fibrosis induction procedure, the day of each biopsy procedure every two weeks, and on the necropsy day before liver tissue harvest. In cohort 2, biopsies past 8-weeks were accompanied with serum

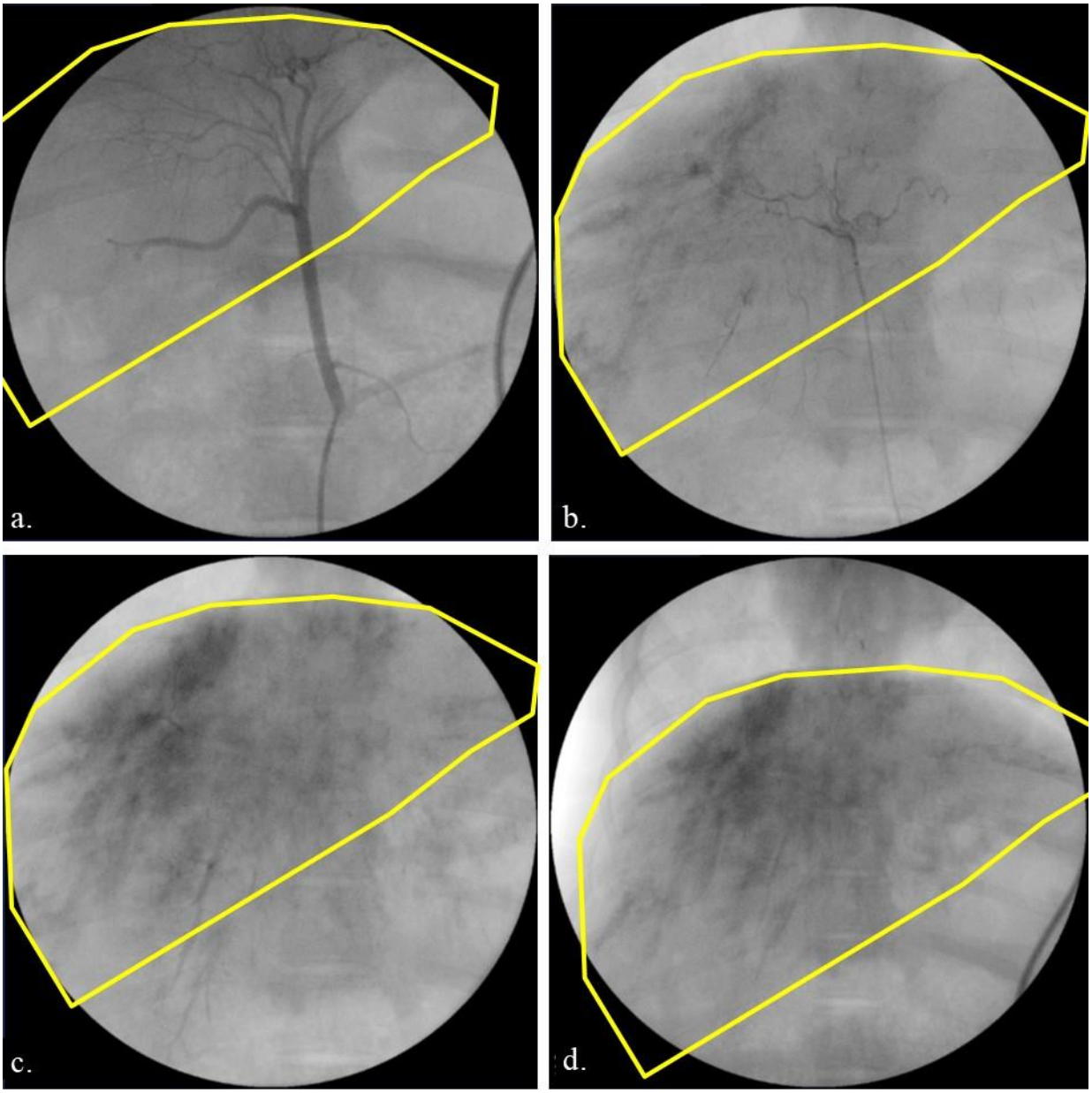

Figure 7 Representative images from fibrosis induction procedure (fluoroscopic images) of PG 5601. Time lapse series of obtained during and after administration of ethanol and ethiodized oil emulsion. (a) shows the hepatic arterial circulation (liver outlines in yellow), as infiltrated by radiopaque contrast, only, during the initial stages of the infiltration procedure. (b)-(d) demonstrates radiopacity of hepatic circulation representing progressive and active infiltration of radiopaque-containing ethanol and ethiodized oil through liver with (d) showing radiopacity of hepatic circulation at periphery of liver after the emulsion was permitted to settle. The yellow outline represents an approximation of the liver borders.

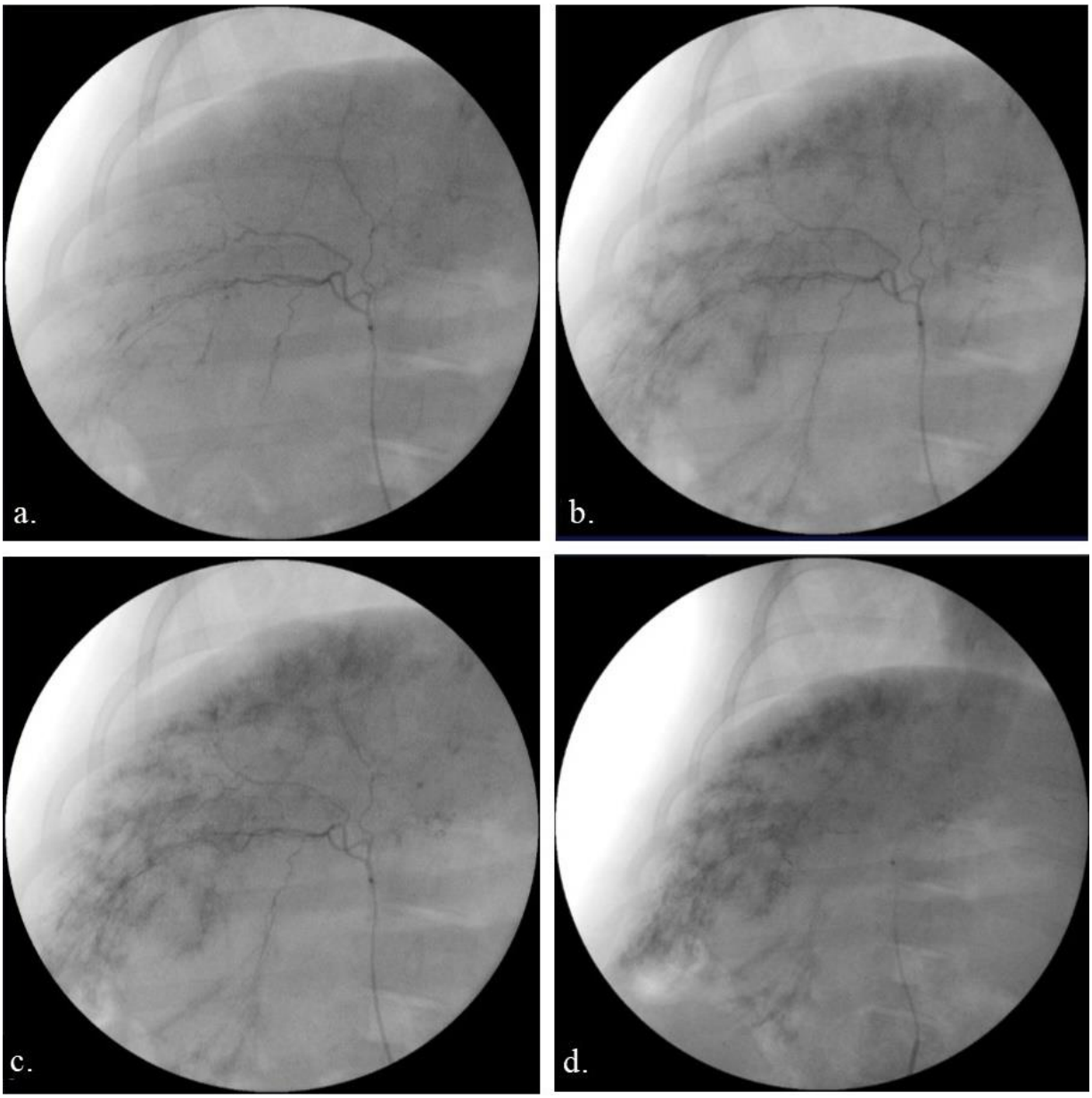

Figure 8 Representative images from fibrosis induction procedure (fluoroscopic images) of PG 5603. (a) conventional porcine hepatic arteries. (b) obtained after administration of ethanol and ethiodized oil emulsion; demonstrates radiopacity of hepatic circulation representing infiltration of radiopaque-containing ethanol and ethiodized oil through liver.

In the control cohort, vital signs, complete metabolic panel, complete blood chemistry and differential, coagulation profile, and liver function tests were acquired on the necropsy day before liver tissue harvest. laboratory collection until 12-weeks.

e. Tissue Processing

This section will review the protocol for tissue collection after the biopsy procedure, and subsequent processing the resulted into histological analysis in the form of METAVIR, percent fibrosis, and inflammation score, as is used in human histological analysis.

i. Sample Collection

After a 3-4 2-cm in length biopsy cores were acquired from during the biopsy procedure, they were placed in 10% neutral formalin fixation solution, the first of many steps for histological sectioning and staining.

ii. Histology Core Preparation of Slides

Formalin fixed liver samples were embedded in paraffin, sectioned at 4-micron thickness, and mounted onto glass slides (Star Frost Plus; Mercedes Medical, Sarasota FL). Slides were processed with routine dehydration and staining procedure using hematoxylin and eosin (H&E), which stains for cellular nuclei and eosinophilic structures such as cytoplasm, and Masson's trichrome, which stains for cytoskeletal proteins such as keratin that is present in fibrosis. H&E is the classical stain utilized by pathologists for histological analysis of basic cellular structure and morphology. Masson's trichrome is the stain utilized in the histological analysis of liver biopsies for liver disease staging with regards to presence of fibrosis and percentage of fibrosis.

f. Histology Assessment

Histological assessment was performed in a blinded fashion by providing unlabeled digital slides to a board certified veterinary pathologist (D.P.R.) with 6 years of experience, housed off-site from the experimental procedure and animal housing.

i. Pathologic Assessment of Slides Utilizing Porcine Fibrosis and Inflammation Scoring System

Qualitative descriptive and semi-quantitative histopathological analyses were in a blinded fashion with the veterinary pathologist unaware at the time of analysis of which treatment group each slide originated from. Before analysis, a METAVIR inflammation grading schematic was prepared for use on porcine histopathological analysis. Once biopsy samples were prepared, they were scanned into digital form using a Hamamatsu Nanozoomer scanner (Hamamatsu Photonics, Hamamatsu Japan), and digital images were visualized using NDP.view2 software (Hamamatsu) and graded for inflammation score, fibrosis score, and percent fibrosis, according to the swine modified METAVIR scoring system (Table I and II)(Huang et al. 2014; Bedossa and Poynard 1996). Digital images of trichrome stained slides were also imported to NIH's ImageJ(Eliceiri et al. 2012) using BioFormats (Linkert et al. 2010), and subjected to color deconvolution for quantification of trichrome positive collagen, expressed as a percentage of total liver tissue section area

TABLE II SWINE MODIFIED METAVIR FIBROSIS GRADING SCHEME

Grade	Qualitative Description
F0	Normal porcine liver; no increase in fibrosis
F1	Mild fibrous expansion of portal areas and/or mild thickening/expansion of few random segments of normal pre-existing fibrous septa
F2	Mild to moderate fibrous expansion of portal tracts and multiple, random, noncontiguous segments of normal fibrous septa surrounding multiple hepatic lobules ± presence of thin bands of fibrosis extending from septa or portal tracts into adjacent lobular parenchyma
F3	Moderate to marked fibrous expansion of contiguous segments of fibrous septa surrounding multiple hepatic lobules; fibrous expansion can involve contiguous segments of septa, and partially encircle hepatic lobules, but typically does not completely circumscribe lobules. Presence of fibrous connective tissue which dissects into lobular parenchyma, surrounding and separating cords of hepatocytes
F4	Cirrhosis; normal fibrous septa surrounding hepatic lobules are expanded by moderate to marked amounts of fibrous connective tissue, with some portal bridging, and frequent dissection into adjacent lobular parenchyma, and separation of hepatic cords. Fibrous connective tissue often completely circumscribes multiple hepatic lobules, which appear irregular/shrunken

TABLE III SWINE MODIFIED METAVIR INFLAMMATION GRADING SCHEME

Activity Score	Portal Inflammation/interface hepatitis	No. of lobular necro-inflammatory foci
A0	None/within normal limits	None
A1		At least 1 per lobule
A2		Several per lobule
A1	Mild to Moderate	None
A2		At least 1 per lobule
A2	Moderate with multifocal interface hepatitis	None
A3		At least 1 per lobule
A3	Moderate to severe with marked interface hepatitis	Any amount

g. Statistical Methods

Statistical analysis for serum vital signs and body measurements, laboratory value, and histopathological grading were compared between pooled experimental cohorts 1 and 2 versus age-matched controls. When experimental cohorts versus control cohorts are compared, pooled parameters that are used for testing are provided in tables, as well as the control cohort parameters they are tested against. All statistical analyses were performed using JMP (JMP Pro 13.0.0. SAS Institute Inc., Cary, NC, 2016). P-value ≤0.05 was considered statistically significant and P-values between 0.05 and 0.1. are considered to be "trending towards" a difference.

i. Vital Signs and Body Measurement Statistical Analysis

Distribution analysis was done for each cohort, showing mean and standard deviation in each cohort for weight, pulse rate, systolic blood pressure, diastolic blood pressure, and mean arterial pressure.

At baseline (0-weeks), average weight between experimental cohort 1 versus experimental cohort 2 were compared using a 2-tailed student t-test. At 8-weeks, pooled experimental cohorts and control cohort weights were compared using a 2-tailed student t-test to evaluate for difference, and 1-tail to assess which direction the difference in means trended towards.

ii. Laboratory Statistical Analysis

For continuous variables, a 2-tailed student's t-test was performed: sodium, potassium, glucose, creatinine, blood urea nitrogen, hemoglobin, white blood cell count, platelets, prothrombin time, partial thromboplastin time, total protein, albumin/globulin ratio, albumin, globulin, alkaline phosphatase, total bilirubin, aspartate aminotransferase, alanine aminotransferase, and gamma-glutamyl aminotransferase. Pooled experimental cohort 1+2 were compared to control cohort at 8-weeks for all values. Any differences in mean were considered statistically significant if P-value < 0.05 and considered to be "trending towards" a difference if P-value <0.10 but >0.05.

iii. Histological Statistical Analysis

For percent fibrosis, a continuous variable, a 2-tailed student's t-test was performed compare the pooled experimental cohort 1+2 to the control cohort at 8-weeks. Any differences in mean were considered statistically significant if P-value < 0.05 and considered to be "trending towards" a difference if P-value <0.10 but >0.05.

For METAVIR Fibrosis grade and METAVIR Inflammation grade, a non-continuous ordinal variable, the Wilcoxon-Mann-Whitney test or the Kruskal-Wallis one-way analysis of variance (ANOVA) test was performed to compare the experimental cohort 1 with experimental cohort 2 at 8-weeks, and also compare cohort 2's most severe score with their score at 20-weeks. Any differences in mean were considered statistically significant if P-value < 0.05 and considered to be "trending towards" a difference if P-value <0.10 but >0.05.

h. Overall Evaluation of Fibrosis

Overall evaluation of fibrosis was done by integrating all three main measures of outcome: clinical exam, serum laboratory values, and histological assessment and grading. Generally, abnormal symptomatology related to liver disease found on clinical exam can be correlated with a serum laboratory abnormality. Normal serum laboratory values in the OCM have not been established, and

therefore assessment of normality and abnormality mainly rely upon known normal ranges for swine(Fielder 2010; Potbellied et al. 2017) and known normal ranges of the clinical examination.

IV. RESULTS

Results were obtained starting at 0-weeks and obtained bi-weekly with each vital sign value, serum laboratory value collected, and associated biopsy tissue sample, up to the final necropsy, where all the same parameters were also collected.

a. Procedure Results

The study cohorts included 5 female Oncopigs in experimental cohort 1, 5 female Oncopigs in experimental cohort 2, and 5 female Oncopigs in the control cohort. In all groups, there was a total of 15 female Oncopigs with mean weight 13.18 kg, range 11-14 kg and no significant difference between the pooled experimental cohorts (1 + 2) and the control cohort (*P-value*=0.06). Technical success was achieved in all experimental cases in cohort 1 and 2 (10/10, 100%). A median of 9 mL of lipiodol:ethanol emulsion (range 8 – 10 mL) administered. The results of the induction procedures are summarized in Table III below.

i. Average Dose Administered

Weight-based dosing for fibrosis induction procedure required weight-based dosing of lipiodol:ethanol emulsion, which was done utilizing weight at baseline, or 0-weeks. Body weights for age-matched controls at time of fibrosis induction procedure were not collected as they did not undergo induction procedure that day. Weight-based dosage was calculated using 0.75 mL of lipiodol:ethanol emulsion per kilogram. Dosing per animal is shown in Table III.

ii. Size, Flow, and Anatomic Site of Infiltration

In cohort 1, there was complete infusion of the lipiodol:ethanol emulsion through the hepatic artery. In cohort 2, there was only incomplete infusion of one subject, PG5600, but the other 4 subjects had complete infusion of the lipiodol:ethanol emulsion via the hepatic artery. For both groups, the goal of the procedure was to deliver the lipiodol:ethanol emulsion at the proper hepatic artery for maximal hepatic infiltration.

TABLE IV VOLUME OF INFUSED LIPIODOL:ETHANOL EMULSION ADMINISTERED PER ANIMAL IN BOTH COHORTS AND CONTROL GROUP

Cohort	Animal No.	Wght (kg)	Ethiodized Oil Volume (mL)
1	PG921	16.2	12
1	PG925	15.9	12
1	PG993	–	12
1	PG994	18.2	–
1	PG995	–	12
2	PG5599	14.2	10
2	PG5600	13.8	6
2	PG5601	11.7	8
2	PG5602	12.4	9
2	PG5603	11.7	9
Control	PG112	–	–
Control	PG113	–	–
Control	PG996	–	–
Control	PG997	–	–
Control	PG998	–	–

b. Laboratory Values

This includes baseline fibrosis assessment, interim values, and final values and how they relate to fibrosis assessment. These include vitals and body measurements, complete metabolic panel, complete blood chemistry, coagulation profile, and liver function tests. The following are a summary of the laboratory outcomes as recorded over time for the pooled experimental cohort of 10-pigs. Summary table of relevant vitals, electrolytes panel, complete blood count, liver function panel, and coagulation panel includes means and standard deviations for the following timepoints: induction(0-weeks), 2-weeks, 4-weeks, 6-weeks, 8-weeks, and necropsy.

i. Vitals and Body Measurements

Weight was documented for cohort 1 and the control group at 8-weeks. Vital signs and body measurements were recorded for cohort 2 at each procedure: induction, biopsies, and necropsy. Vitals and body measurement averages and standard deviations by cohort are shown in Table IV.

In experimental cohort 1, a total of 5 female pigs were weighed before induction procedure and on the day of necropsy. In experimental cohort 2, a total of 5 female pigs were weighed before induction procedure, bi-weekly on the day of each biopsy procedure, and on the day of necropsy.

At 8-weeks, comparison of pooled experimental cohorts 1 + 2 mean weight versus the control cohort mean weight showed that there was no statistically significant difference between mean weights (*P-value*= 0.11, 2-tail).

Pulse rate for cohort 1 and the control cohort were not recorded. In experimental cohort 2, a total of 5 female pigs had pulse rate recorded before and during induction procedure, bi-weekly on the day of each biopsy procedure, and on the day of necropsy. Normal Swine pulse rate at this age ranges from 80 beats per minutes (bpm) to 130 bpm at this age. There was no significant deviation from the normal range and pulse rate mean tended to decrease from baseline to 20-weeks, which is expected as the Oncopigs mature from piglet to adolescence.

Blood pressure for cohort 1 and the control cohort were not recorded. In experimental cohort 2, a total of 5 female pigs had blood pressure before and during induction procedure, bi-weekly on the day of each biopsy procedure, and on the day of necropsy.

Normal range of systolic blood pressure in swine is 100-120 mmHg. At 0-weeks, cohort 2 mean systolic blood pressure was within normal limits. At 4-, 6-, and 8-, and 20-weeks (necropsy), there was a steady increase in blood pressure to above the normal limit of normal systolic blood pressure, from a mean of 147 mmHg at 4-weeks to a mean of 218 mmHg at 20-weeks, indicating hypertension.

Normal range of diastolic blood pressure in swine is 70-90 mmHg. At 0-, 4-, 6-, and 8-weeks, cohort 2 mean diastolic blood pressure was below the normal range. At 20-weeks (necropsy), mean diastolic blood pressure in cohort 2 was within the normal range of diastolic blood pressure.

Normal range of mean arterial pressure (MAP) in swine is not known. In cohort 2, mean

TABLE V BODY MEASUREMENTS ACROSS GROUPS[a,]

Measure	Cohort 1 (stdev)	Cohort 2 (stdev)	Control (stdev)	P-Value
Weight				
Baseline	16.8 (1.25)	13.2 (1.1)	–	
4-weeks	–	22.6 (6.7)	–	
6-weeks	–	28.1 (7.3)	–	
8-weeks	36.0 (5.9)	34.2 (4.3)	38.2 (0.9)	
	35.1 (4.9)			0.11**
20-weeks	–	52.8 (4.0)	–	
Pulse Rate				
Baseline	–	124.8 (14.5)	–	
4-weeks	–	98.6 (14.6)	–	
6-weeks	–	74.6 (4.8)	–	
8-weeks	–	89 (22.8)	–	
20-weeks	–	77.4 (12.3)	–	
Systolic Blood Pressure				
Baseline	–	112.6 (23.4)	–	
4-weeks	–	147.4 (31.7)	–	
6-weeks	–	158.6 (11.8)	–	
8-weeks	–	167 (24.4)	–	
20-weeks	–	218.6 (17.7)	–	
Diastolic Blood Pressure				
Baseline	–	55.6 (22.0)	–	
4-weeks	–	64.0 (26.6)	–	
6-weeks	–	68.6 (28.0)	–	
8-weeks	–	66.4 (25.8)	–	
20-weeks	–	80.5 (33.7)	–	
Mean Arterial Blood Pressure				
Baseline	–	78.9 (17.2)	–	
4-weeks	–	96.2 (26.3)	–	
6-weeks	–	105.5 (5.6)	–	
8-weeks	–	105.5 (18.4)	–	
20-weeks	–	134.7 (24.0)	–	

a Body Measurements across groups at time baseline , 4-weeks, 6-weeks, 8-weeks, and 20-weeks
** = 2-tail significance

MAP was at 78 mmHg at baseline, and increased to 135 mmHg at necropsy.

ii. Complete Metabolic Panel

A complete metabolic panel drawn from serum samples was recorded for cohort 1 at 0-, 4-, 6-, and 8-weeks, and the control group at 8-weeks. A complete metabolic panel drawn from serum samples was recorded for cohort 2 at each procedure: induction, biopsies, and necropsy. Complete metabolic panel averages and standard deviations by cohort are shown in Table V.

Normal range for swine serum sodium is 135-150 mmol/L. In a comparison of serum sodium at 8-weeks of pooled experimental cohorts 1+2 (mean=141.6, stddev=2.4) versus control cohort (mean=142.0; stddev=3.4), there was no significant difference between experimental and control groups (*P-value*=0.82; 2-tail).

Normal range for swine serum potassium is 4.4-6.7 mmol/L. In a comparison of serum potassium at 8-weeks of pooled experimental cohorts 1+2 (mean=4.6, stddev=1.2) versus control cohort (mean=5.5; stddev=1.1), there was no significant difference between experimental and control groups (*P-value*=0.19; 2-tail).

Normal level for swine serum glucose is approximately 110 mg/dL. In a comparison of serum glucose at 8-weeks of pooled experimental cohorts 1+2 (mean=91.4, stddev=12.6) versus control cohort (mean=136.0; stddev=22.6), there was no significant difference between experimental and control groups (*P-value*=0.08; 2-tail). While the control cohort appears to trend towards a higher average serum glucose level, without a strictly monitored eating schedule, or the gold-standard glucose tolerance test, a higher average glucose level has no clinical significance, especially within the clinical picture of this fibrosis model which may impair glucose-related metabolism. Statistically, this is especially evident by the large standard deviation of the control cohort.

TABLE VI COMPLETE METABOLIC PANEL OF ALL COHORTS[a, b]

Serum Laboratory	Cohort 1 (stdev)	Cohort 2 (stdev)	Control (stdev)	P-value
Sodium (mmol/L)				
Baseline	138.4 (0.90)	139.8 (1.3)	–	
4-weeks	147.0 (1.8)	138.6 (1.7)	–	
6-weeks	144 (2.9)	139.2 (1.6)	–	
8-weeks	141.3 (3.1)	141.8 (2.3)		
	141.6 (2.4)		142.0 (3.4)	0.82[b]
20-weeks	–	139.3 (1.5)	–	–
Potassium (mmol/L)				
Baseline	3.9 (0.3)	3.7 (0.8)	–	
4-weeks	6.8 (1.6)	3.94 (0.2)	–	
6-weeks	5.5 (0.7)	4.08 (0.9)	–	
8-weeks	5.8 (1.1)	3.8 (0.3)	5.5 (1.1)	
	4.6 (1.2)			0.19 [b]
20-weeks	–	3.9 (0.2)	–	–
Glucose (mg/dL)				
Baseline	106 (19.0)	101.0 (19.1)	–	
4-weeks	133.2 (41.6)	112.86 (16.0)	–	
6-weeks	88.5 (22.4)	112.6 (19.0)	–	
8-weeks	96.0 (15.7)	88.6 (10.4)		
	91.4 (12.1)		136 (22.6)	0.008**
20-weeks	–	111.0 (5.6)	–	–
Creatinine (mg/dL)				
Baseline	0.62 (0.8)	0.68 (0.07)	–	
4-weeks	0.96 (0.9)	0.93 (0.1)	–	
6-weeks	0.85 (0.06)	0.93 (0.1)	–	
8-weeks	0.83 (0.06)	0.97 (0.1)		
	0.92 (0.1)		0.84 (0.1)	0.29[b]
20-weeks	–	1.4 (0.06)	–	
Blood Urea Nitrogen (mg/dL)				
Baseline	12.0 (2.3)	6.0 (1.4)	–	
4-weeks	13.4 (2.4)	9.4 (2.1)	–	
6-weeks	11.3 (2.6)	4.8 (0.84)	–	
8-weeks	10.3 (2.3)	5.4 (0.9)		
	7.3 (2.9)		13.4 (1.5)	0.0004**
20-weeks	–	10.7 (1.2)	–	–

a Complete Metabolic Panel of Cohort 1, Cohort 2, and Control Cohort at Baseline (week-0), 4-weeks, 6-weeks, 8-weeks, and 20-weeks
b = denotes a 2-tail test versus a 1-tail test
**=2-tail significance

Normal range for swine serum creatinine is 1.0-2.7 mg/dL. In a comparison of serum creatinine at 8-weeks of pooled experimental cohorts 1+2 (mean=0.92, stddev=0.1) versus control cohort (mean=0.84; stddev=0.1), there was a significant difference between experimental and control groups (*P-value*=0.0002, 1-tail; *P-value*=0.0004, 2-tail) with the control cohort having a higher average creatinine.

Normal range for swine serum blood urea nitrogen (BUN) 10-30 mg/dL. In a comparison of serum BUN at 8-weeks of pooled experimental cohorts 1+2 (mean=7.3, stddev=2.9) versus control cohort (mean=13.4; stddev=1.5), there was no significant difference between experimental and control groups (*P-value*=0.19; 2-tail). While the control cohort appears to have a significantly higher average BUN, it is still within normal range for BUN values.

iii. Complete Blood Count

A CBC drawn from serum samples was recorded for cohort 1 at 0-, 4-, 6-, and 8-weeks, and the control group at 8-weeks. A complete blood count (CBC) drawn from serum samples was recorded for cohort 2 at each procedure: induction, biopsies, and necropsy. In the control cohort, 2 animals (PG112 and PG996) did not have all values in the CBC because the samples coagulated before analysis and, therefore, were not included in the analysis. Complete blood count averages and standard deviations by cohort are shown in Table VI.

Normal range for swine hemoglobin is 10-16 g/dL. In a comparison of hemoglobin at 8-weeks of pooled experimental cohorts 1+2 (mean=12.7, stddev=1.8) versus control cohort (mean=14.3; stddev=0.3), there was a significant difference between experimental and control groups (*P-value*=001, 1-tail; *P-value*=0.02, 2-tail). However, because both the pooled experimental cohort and control cohort had mean hemoglobin within normal range, there is no clinical or pathological difference between the two groups.

TABLE VII COMPLETE BLOOD COUNT OF ALL COHORTS[a, b,]

Serum Laboratory	Cohort 1 (stdev)	Cohort 2 (stdev)	Control (stdev)	P-value
Hemoglobin (g/dL)				
Baseline	10.2 (0.5)	10.9 (0.5)	–	
4-weeks	14.3 (0.6)	11.2 (0.7)	–	
6-weeks	13.2 (–)	11.0 (0.4)	–	
8-weeks	14.3 (0.4)	11.1 (0.4)	14.3 (0.3)	
	12.7 (1.8)			0.02**
20-weeks	–	11.2 (0.3)	–	–
White Blood Cell Count (x 10^3/µL)				
Baseline	14.1 (3.6)	20.9 (14.8)	–	
4-weeks	24.0 (2.0)	11.3 (3.6)	–	
6-weeks	20.9 (–)	11.5 (2.2)	–	
8-weeks	21.4 (4.1)	10.5 (1.2)	15.6 (1.8)	
	16.0 (6.4)			0.87[b]
20-weeks	–	10.7 (2.0)	–	–
Platelets (x 10^3/µL)				
Baseline	546.8 (69.2)	319.2 (126.6)	–	
4-weeks	715.2 (87.4)	332.4 (59.6)	–	
6-weeks	599.0 (–)	327.0 (43.7)	–	
8-weeks	580.6 (155.7)	324.0 (49.9)	502.7 (46.7)	
	452.3 (173.4)			0.42[b]
20-weeks	–	317.0 (30.3)	–	–

a Complete Blood Count of Cohort 1, Cohort 2, and Control Cohort at Baseline (week-0), 4-weeks, 6-weeks, 8-weeks, and 20-weeks
b = denotes a 2-tail test versus a 1-tail test
**=2-tail significance

Normal range for swine white blood cell (WBC) count is 11-22 x 10^3/µL. In a comparison of white blood cell count at 8-weeks of pooled experimental cohorts 1+2 (mean=16.0, stddev=6.4) versus control cohort (mean=15.6; stddev=1.8), there was no significant difference between experimental and control groups (*P-value*=0.87; 2-tail).). Additionally, because both the pooled experimental cohort and control cohort had mean WBC within normal range, there is no clinical or pathological difference between the two groups.

The swine subjects mounted an appropriate immunological response to the toxic insult of the lipiodol:ethanol emulsion, similar to what is observed in humans after hepatic toxic insult. However,

this WBC relative elevation observed from the beginning and therefore, the interpretation and utility of this measure is unknown. This is likely a normal variant observed in young piglets.

Normal range for swine platelets is 200-500 x $10^3/\mu L$. In a comparison of platelets at 8-weeks of pooled experimental cohorts 1+2 (mean=452.3, stddev=173.4) versus control cohort (mean=502.7; stddev=46.7), there was no significant difference between experimental and control groups (*P-value*=0.42; 2-tail). Statistically, this is expected because, just like in humans, the swine platelet values differ widely from individual to individual, and are still be within their normal range.

iv. Coagulation Profile

A complete blood chemistry drawn from serum samples was recorded for cohort 1 at 0-, 4-, 6-, and 8-weeks, and the control group at 8-weeks. A complete blood chemistry drawn from serum samples was recorded for cohort 2 at each procedure: induction, biopsies, and necropsy. In the control cohort, 1 animal (PG994) did not have coagulation profile values because with the sample acquired "testing could not be performed", therefore, were not included in the analysis. Coagulation profile averages and standard deviations by cohort are shown in Table VII.

Normal range for prothrombin time (PT) is unknown, but our animal laboratory sets a normal at 12.5 seconds. In a comparison of PT at 8-weeks of pooled experimental cohorts 1+2 (mean=13.0, stddev=0.6) versus control cohort (mean=13.1; stddev=0.7), there was no significant difference between experimental and control groups (*P-value*=0.73; 2-tail).

Normal range for swine partial thromboplastin time (PTT) is unknown, but our laboratory sets a normal at 25.6 sec. In a comparison of PTT at 8-weeks of pooled experimental cohorts 1+2 (mean=10.9, stddev=2.0) versus control cohort (mean=11.9; stddev=2.7), there was no significant difference between experimental and control groups (*P-value*=0.53; 2-tail).

TABLE VIII COAGULATION PROFILE OF ALL COHORTS[a, b]

Serum Laboratory	Cohort 1 (stdev)	Cohort 2 (stdev)	Control (stdev)	P-value
Prothrombin Time (secs)				
Baseline	13.5 (0.7)	12.2 (0.6)	–	
4-weeks	13.2 (0.8)	11.7 (1.4)	–	
6-weeks	12.9 (0.5)	12.7 (1.4)	–	
8-weeks	12.9 (0.5)	13.1 (0.7)	13.1 (0.7)	
	13.0 (0.6)			0.73[b]
20-weeks	–	12.2 (1.1)	–	–
Partial Thromboplastin Time(secs)				
Baseline	13.5 (1.2)	8.6 (1.8)	–	
4-weeks	12.8 (1.3)	14.2 (10.2)	–	
6-weeks	13.9 (0.7)	7.7 (0.6)	–	
8-weeks	13.6 (2.0)	8.2 (0.3)	11.9 (2.7)	
	10.9 (3.2)			0.53[b]
20-weeks	–	8.7 (0.9)	–	–

a Coagulation Profile of Cohort 1, Cohort 2, and Control Cohort at Baseline (week-0), 4-weeks, 6-weeks, 8-weeks, and 20-weeks
b = 2-tail test

v. Liver Function Profile

A complete liver function profile was drawn from serum samples and recorded for cohort 1 at 0-, 4-, 6-, and 8-weeks, and the control group at 8-weeks. A complete liver function profile was drawn from serum samples and recorded for cohort 2 at each procedure: induction, biopsies, and necropsy. In the control cohort, 1 animal (PG994) did not have coagulation profile values because with the sample acquired "testing could not be performed", therefore, were not included in the analysis. In cohort 1 and the control cohort, alanine aminotransferase (ALT) was not drawn at any timepoint. In cohort 2, complete liver function profile did not start including GGT in Cohort 2 until week 10. Cohort 2's 10-week value was used as a surrogate for 8-weeks comparison. Liver function profile averages and standard deviations by cohort are shown in Table VIII.

Normal range for swine total protein is 7.9-8.9 g/dL. In a comparison of serum total protein

TABLE IX LIVER FUNCTION PROFILE OF ALL COHORTS[a, b, c]

Serum Laboratory	Cohort 1 (stdev)	Cohort 2 (stdev)	Control (stdev)	P-value
Total Protein (g/dL)				
Baseline	5.0 (0.2)	4.8 (0.3)	–	
4-weeks	6.7 (1.0)	5.1 (0.2)	–	
6-weeks	5.7 (0.3)	5.5 (0.2)	–	
8-weeks	5.9 (0.2)	5.7 (0.2)		
	5.8 (0.2)		5.0 (1.0)	0.16++
20-weeks	–	5.7 (0.2)	–	–
Albumin/Globulin Ratio				
Baseline	1.94 (0.3)	2.3 (0.3)	–	
4-weeks	1.5 (0.3)	2.1 (0.2)	–	
6-weeks	1.9 (0.1)	1.5 (0.1)	–	
8-weeks	1.6 (0.3)	1.8 (0.1)		
	1.7 (0.2)		1.8 (0.2)	0.6++
20-weeks	–	2.1 (0.2)	–	–
Albumin (g/dL)				
Baseline	3.3 (0.1)	3.4 (0.1)	–	
4-weeks	4.0 (0.3)	3.6 (0.2)	–	
6-weeks	3.7 (0.2)	3.3 (0.2)	–	
8-weeks	3.6 (0.3)	3.6 (0.1)	3.7 (0.2)	
	3.6 (0.2)			0.4++
20-weeks	–	3.8 (0.2)	–	–
Globulin (g/dL)				
Baseline	1.7 (0.2)	1.4 (0.2)	–	
4-weeks	2.7 (0.7)	1.7 (0.1)	–	
6-weeks	2.0 (0.2)	2.2 (0.1)	–	
8-weeks	2.3 (0.2)	2.1 (0.2)	2.1 (0.2)	
	2.2 (0.2)			0.91++
20-weeks	–	1.8 (0.1)	–	–
Alkaline Phosphatase (mg/dL)				
Baseline	101.6 (1.7)	264.4 (17.7)	–	
4-weeks	102.8 (1.8)	175.0 (28.4)	–	
6-weeks	103.0 (2.8)	185.8 (29.4)	–	
8-weeks	117.0 (23.6)	191.8 (33.0)	164.2 (23.4)	
	154.4 (47.8)			0.6++
20-weeks	–	148.7 (22.0)	–	–
Total Bilirubin (mg/dL)				
Baseline	0.58 (0.2)	0.18 (0.09)	–	
4-weeks	0.1 (0.0)	0.12 (0.2)	–	
6-weeks	0.1 (0.0)	0.14 (0.05)	–	
8-weeks	0.14 (0.09)	0.17 (0.1)	0.14 (0.05)	
	0.16 (0.1)			0.70++
20-weeks	–	0.1 (0.03)	–	–
Aspartate Aminotransferase (U/L)				
Baseline	42.0 (8.6)	46.0 (16.0)	–	

TABLE IX LIVER FUNCTION PROFILE OF ALL COHORTS (CONTINUED)

Serum Laboratory	Cohort 1 (stdev)	Cohort 2 (stdev)	Control (stdev)	P-value
4-weeks	39.4 (16.5)	36.8 (21.1)	–	
6-weeks	29.0 (8.6)	63.6 (67.5)	–	
8-weeks	39.4 (20.8)	20.0 (2.9)	33.4 (8.2)	
	29.7 (17.3)			0.6[c]
20-weeks	–	15.0 (2.6)	–	–
Alanine Aminotransferase (U/L)				
Baseline	–	25.2 (4.3)	–	–
4-weeks	–	24.0 (2.2)	–	–
6-weeks	–	25.6 (4.2)	–	–
8-weeks	–	23.4 (4.1)	–	–
20-weeks	–	23.6 (3.1)	–	–
Gamma-Glutamyl Transferase (U/L)				
Baseline	40.6 (16.5)	–	–	
4-weeks	58.8 (21.5)	–	–	
6-weeks	42.8 (11.1)	–	–	
8-weeks	42.4 (15.2)	31.6 (8.8)[b]	32.3 (3.8)	
	37.0 (4.1)			0.3[c]
20-weeks	–	33.5 (8.1)	–	–

a Liver Function Profile of Cohort 1, Cohort 2, and Control Cohort at Baseline (week-0), 4-weeks, 6-weeks, 8-weeks, and 20-weeks with P-values
b = GGT from 10-weeks, but used for 8-week comparison since closest available data point
c = 2-tail test

at 8-weeks of pooled experimental cohorts 1+2 (mean=5.8, stddev=0.2) versus control cohort (mean=5.0; stddev=1.0), there was no significant difference between experimental and control groups (*P-value*=0.08, 1-tail; *P-value*=0.16, 2-tail).

From the induction procedure at baseline (0-weeks) to the final euthanization date, total proteins produced below the threshold for normal total protein values. This may be due to the young age of these pig. Therefore, a new normal for our OCM total protein can be set at a center of 5.6 g/dL, derived from the control cohort mean, with a range of 3.8-6.2 g/dL, found utilizing the lowest and highest acceptable values for total protein while not violating the null hypothesis.

Normal range for swine albumin/globulin ratio is unknown. In a comparison of albumin/globulin ratio at 8-weeks of pooled experimental cohorts 1+2 (mean=1.7, stddev=0.2) versus control cohort (mean=1.8; stddev=0.2), there was no significant difference between experimental and control groups (*P-value*=0.6; 2-tail). Globulin value at induction procedure at baseline (0-weeks) and the necropsy procedure at 8-weeks were below normal levels. However, normal ratio of albumin to globulin is not known for swine subjects and therefore the clinical significance of these findings are unknown.

Normal range for swine albumin is 3.5-5.7 g/dL L. In a comparison of albumin at 8-weeks of pooled experimental cohorts 1+2 (mean=3.6, stddev=0.2) versus control cohort (mean=2.7; stddev=0.2), there was no significant difference between experimental and control groups (*P-value*=0.4; 2-tail).

Normal range for swine globulin is 5.3-6.4 g/dL. In a comparison of globulin at 8-weeks of pooled experimental cohorts 1+2 (mean=2.2, stddev=0.2) versus control cohort (mean=2.1; stddev=0.2), there was no significant difference between experimental and control groups (*P-value*=0.62; 2-tail). Globulin levels at induction procedure at baseline (0-weeks) and the necropsy procedure at 8-weeks were below normal levels. However, normal globulin level is not known for

swine subjects. This indicates that our OCM may have a different baseline globulin level than established swine values. Therefore, a new normal for our OCM globulin can be set at a center of 2.14 g/dL, derived from the control cohort mean, with a range of 1.9-2.3 g/dL, found utilizing the lowest and highest acceptable values for total protein while not violating the null hypothesis.

Normal range for swine alkaline phosphatase is 118-395 U/L. In a comparison of serum alkaline phosphatase at 8-weeks of pooled experimental cohorts 1+2 (mean=154.4, stddev=47.8) versus control cohort (mean=164.2; stddev=23.4), there was no significant difference between experimental and control groups (*P-value*=0.6; 2-tail).

Normal range for swine total bilirubin is 1.0-10.0 mg/dL L. In a comparison of serum total bilirubin at 8-weeks of pooled experimental cohorts 1+2 (mean=0.16, stddev=0.1) versus control cohort (mean=0.14; stddev=0.05), there was no significant difference between experimental and control groups (*P-value*=0.7; 2-tail). Total protein levels at induction procedure at baseline (0-weeks) and at necropsy procedure at 8-weeks were below normal levels. However, normal total bilirubin level is not known for swine subjects.

Normal range for swine aspartate aminotransferase (AST) is 32-84 U/L. In a comparison of serum AST at 8-weeks of pooled experimental cohorts 1+2 (mean=29.7, stddev=17.3) versus control cohort (mean=33.4; stddev=8,2), there was no significant difference between experimental and control groups (*P-value*=0.6; 2-tail). In cohort 2, AST levels peak at 2-weeks with resolution to normal levels at 8-weeks and subsequently at 20-weeks. There appears to be a significant difference from normal values only at 2-weeks, but the clinical significance of this undulating AST level may be of note for future experiments.

Normal range for swine alanine aminotransferase is 31-55 U/L. Only cohort 2 had serum ALT levels drawn. Throughout the experiment, ALT levels remained below the normal range for serum ALT. Therefore, the normal range for ALT may be different in the OCM.

Normal range for swine serum gamma-glutamyl transferase (GGT) is 10-60 U/L. In a comparison of serum sodium at 8-weeks of pooled experimental cohorts 1+2 (mean=37.0, stddev=4.1) versus control cohort (mean=32.3; stddev=3.8), there was no significant difference between experimental and control groups (*P-value*=0.32; 2-tail). In cohort 2, GGT levels peak at 2-weeks after fibrosis induction, with resolution to normal levels at 4-weeks, persisting to the endpoint at 20-weeks.

c. Histological Outcome

Histological outcome was assessed by using sectioned liver tissue stained for H&E and Trichrome. In all samples, H&E stain was used to evaluate liver parenchymal microarchitectures, and Masson's Trichrome stain was used to evaluate for fibrotic discription of sinusoudal liver architecture. All tissue was evaluated (Table IX) using the swine-adapted METAVIR Fibrosis and Inflammation grading scheme (Table X and XI).

In cohort 1, gross anatomic inspection of liver sections included both normal and abnormal appearing liver on the day of the necropsy procedure (Fig. 9). On histopathological assessment at 8-weeks post-induction, macronodular liver fibrosis was heterogeneously appreciated in areas of both fibrosis and normal parenchyma in cohort 1 subjects (Table X).

At 8-weeks post-induction, there was significant fibrosis in all 5 subjects (Fig. 9). Histopathological findings in this cohort showed isolated extensive foci of moderate to marked fibrous expansion of pre-existing fibrous septa and expanding portal tracts. Inflammatory cells of primarily lymphocytes and plasma cells, with fewer pigment-laden macrophages, and rare eosinophils, were found to be interspersed among several multifocalities of fibrous tissue and infiltrating portal and septal tracts. There was common disruption of the limiting plate and dissection into adjacent lobular parenchyma due to portal inflammation and fibrosis. Often, there

were partially or completely encircled hepatic lobules, appearing small and irregular, which contained swollen hepatocytes undergoing lipid-type vacuolar degeneration.

Effectiveness of fibrosis induction in cohort 1 was 100% (5/5) (Table X). At 8-weeks, the METAVIR fibrosis score for abnormal, fibrotic-appearing liver tissue from experimental cohort 1 (median F3, range F2-F4; Fig. 10) was significantly higher (P = 0.0013; 2-tail) than both normal-appearing liver tissue from experimental cohort 1 (median F0, range F0-F1) and liver tissue from the control cohort (median F0, range F0-F1) (Fig. 11). In terms of inflammation, abnormal-appearing fibrotic liver tissue from experimental cohort 1 (median A2, range A2-A3), was also significantly higher (P = 0.0013; 2-tail) than both normal-appearing liver tissue from experimental cohort 1 (median A0, range A0-A1) and healthy liver tissue from the control cohort (median A1, range A0-A1). Quantitative assessment of fibrosis demonstrated a median percent fibrosis of 15.3% (range 5.0-22.9%, std dev) in cohort 1, which was elevated in comparison to all normal liver tissue controls, from both normal-appearing tissue from experimental cohort 1 (median 6.1%, range 2.5-9.4%; P = 0.019) and healthy control pigs (median 8.7%, range 5.8-12.1%. P = 0.064; 2-tail).

In cohort 2, gross anatomic inspection of liver sections demonstrated normal-appearing liver in all cohort 2 pigs at necropsy at 20-weeks post-induction (similar to Fig 9). On histopathological assessment at 8-weeks post-induction, macronodular liver fibrosis was heterogeneously appreciated in areas of both fibrosis and normal parenchyma, but less severe than cohort 1 (Table XI).

Effectiveness of fibrosis induction procedure in cohort 2 was 100% (5/5). In cohort 2, histopathological signs of liver fibrosis were apparent as early as 2-weeks after fibrosis induction procedure (similar to Fig. 12), with median METAVIR fibrosis grade of F2 (range F1-F3), a median

TABLE X HISTOPATHOLOGICAL OUTCOME: PERCENT FIBROSIS, METAVIR FIBROSIS SCORE, METAVIR INFLAMMATION SCORE

	Inflammation at Necropsy	Modified META VIR Score at Necropsy	% Fibrosis-Necropsy	Inflamation Score - 2 wks	Modified META VIR Score - 2 wks	% Fibrosis - 2 wks	Inflamation Score - 4 wks	Modified META VIR Score - 4 wks	% Fibrosis - 4 wks	Inflamation Score - 6 wks	Modified META VIR Score - 6 wks	% Fibrosis - 6 wks	Inflamation Score - 8 wks	Modified META VIR Score - 8 wks	% Fibrosis - 8 wks
PG5599	A1	F2	7.77	A2	2	4.42	A0	F1	7.05	–	–	–	A1	F0	4.88
PG5600	A1	F1	7.21	A2	2	4.3	A1	F1	4.59	A1	F2	4.95	A1	F0	3.51
PG5601	A1	F1	8.74	A2	3	5.81	A1	F2	6.5	A1	F2	8.06	A1	F1	5.69
PG5602	A1	F2	12.3	A1	2	3	A0	F1	4.16	A1	F3	5.57	A1	F1	5.82
PG5603	A1	F2	12.26	A2	1	3.16	A1	F3	5.83	A1	F1	7.79	A1	F0	4.11
PG921	–	–	–	–	–	–	–	–	–	–	–	–	A2	F3	18.4
PG925	–	–	–	–	–	–	–	–	–	–	–	–	A3	F4	19.3
PG993	–	–	–	–	–	–	–	–	–	–	–	–	A2	F3	13.2
PG994	–	–	–	–	–	–	–	–	–	–	–	–	A3	F4	4.98
PG995	–	–	–	–	–	–	–	–	–	–	–	–	A2	F3	15.3

TABLE XI COHORT 1 LIVER HISTOLOGICAL ASSESSMENT

8-weeks	METAVIR Fibrosis Grade	METAVIR Inflammation Grade
PG921	F3	A2
PG925	F4	A3
PG993	F3	A2
PG994	F4	A3
PG995	F3	A2
Median	F3	A2

TABLE XII COHORT 2 LIVER HISTOLOGICAL OUTCOMES

Most Severe	METAVIR Fibrosis Grade		METAVIR Inflamm Grade	
	Most Severe Grade (week)	Grade at 20-weeks	Most Severe Grade (week)	Grade at 20-weeks
PG599	F3 (6-weeks)	F2	A1 (2-weeks)	A1
PG600	F2 (2-weeks)	F2	A2 (2-weeks)	A1
PG601	F3 (18 weeks)	F1	A2 (2-weeks)	A1
PG602	F3 (2-weeks)	F1	A2 (2-weeks)	A1
PG603	F3 (4-weeks)	F2	A2 (2-weeks)	A1
Median	F3	F2	A2	A1

METAVIR inflammation grade of A2 (range A1-A2), and a median percent fibrosis of 8.1% (range 6.6-11.6%) at this time point. During the follow-up period, fibrosis METAVIR grading peaked at median METAVIR grade F3 (range F2-F3) and median METAVIR inflammation grade A2 (range A1-A2, Table XI). However, fibrosis did not persist to the 20-week endpoint, and durability of fibrosis was 0% (0/5). 20-week post-induction liver histology revealed a median METAVIR fibrosis grade of only F2 (range F1-F2), with a relatively reduced median inflammation score, median A1 (Table XI; Figure 13), but with a similar median percent fibrosis as that seen at the 2-weeks timepoint, 8.7% (range 7.4-10.5%). Evaluation of bi-weekly serial liver biopsy specimens from this experimental cohort 2 did not show histopathological evidence of fibrosis with progression, or cirrhosis development. It is important to note that sampling variation due to variable fibrosis foci

resulting from heterogenous infusion of lipiodol:ethanol emulsion during the infusion procedure may be the cause of the observed variation in histopathological results across timepoints.

d. Clinical Impact

Clinically, fibrosis as measured by histology results was transiently achieved but did not persist. There was a potent inflammatory response to the induction procedure, as is classically seen in the chronic hepatitis of alcohol liver disease that progresses to cirrhosis. Because it is known that cirrhosis is a long-term chronic process, this project elucidates what changes in histology and hepatologic function occur in acute to acute-chronic insults with ethanol. It is this acute process summated into a longer chronic cyclical process that culminates into the irreversible state of liver disease fibrosis. The presence of HE or ascites were the two main clinical outcomes that indicated portal hypertension secondary to liver fibrosis. The physical exam of the swine subjects did not result in the presence of a fluid wave, wan indication of abdominal ascites. On ultrasound examination before biopsy procedures, ascited was not appreciated in any of the cohorts.

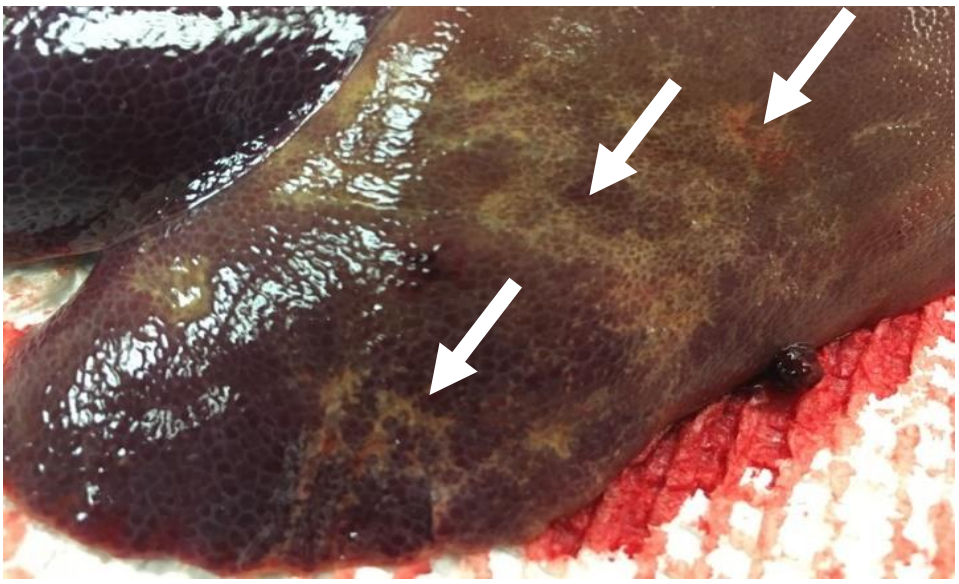

Figure 9 Gross histology of cohort 1 showing areas of normal and fibrotic liver tissue at 8-weeks, with nodularity of the hepatic capsular surface, and enhanced reticular pattern and discoloration (arrows) of hepatic parenchyma, indicative of macronodular fibrosis.

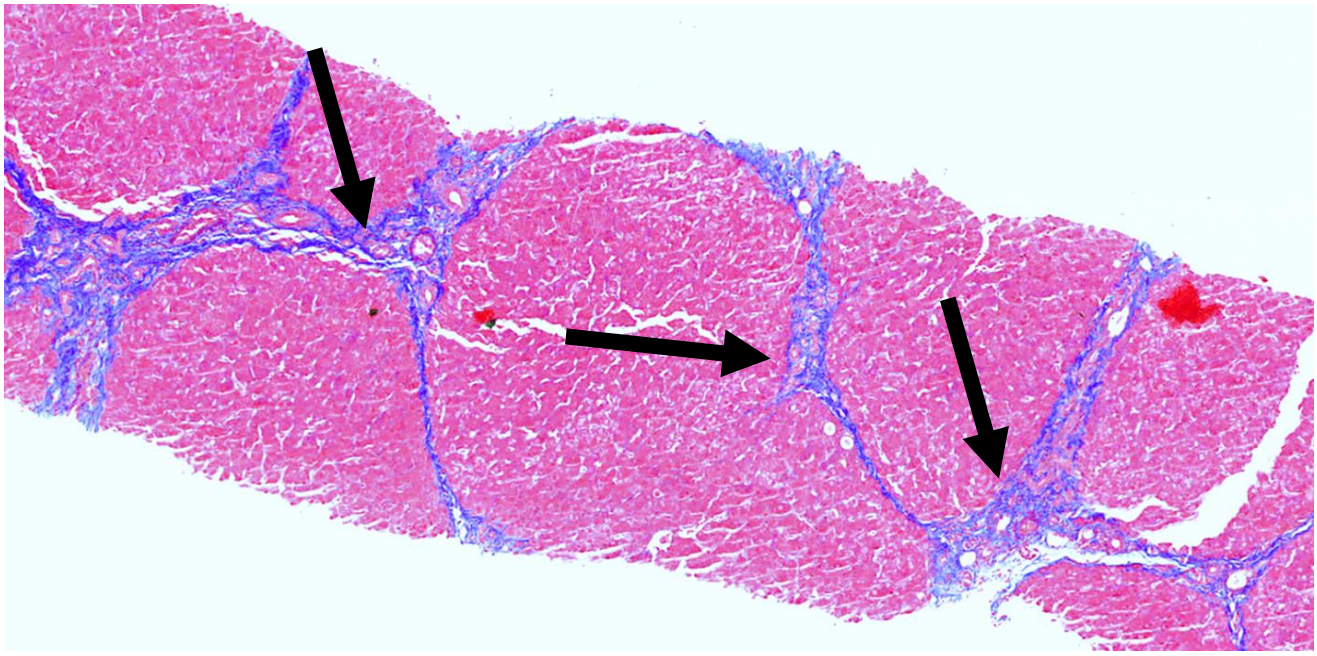

Figure 10 Representative images of Masson's trichrome stain in cohort 2 porcine liver section histologically graded for fibrosis using porcine adapted METAVIR scheme at 5x magnification. This image is of a section of biopsy taken at 2-weeks post-induction demonstrating METAVIR F2 fibrosis grading, characterized by moderate fibrous expansion of portal areas and preexisting septa (arrows).

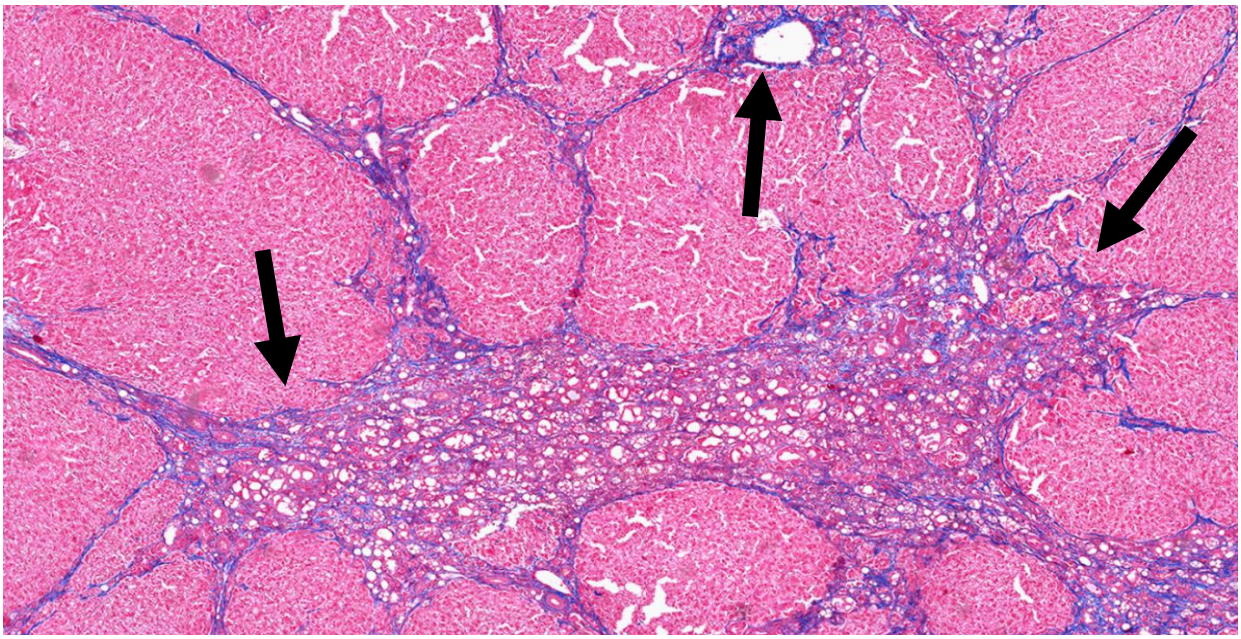

Figure 11 Representative images of Masson's trichrome stain in cohort 1 porcine liver section histologically graded for fibrosis using porcine adapted METAVIR, 5x magnification. This image is 8-weeks post-induction demonstrating METAVIR F3 grading, with portal areas showing expansion and fibrous septa with abundant amounts of blue fibrosis (arrows) which extends into adjacent lobular parenchyma and surround and separates hepatocyte clusters.

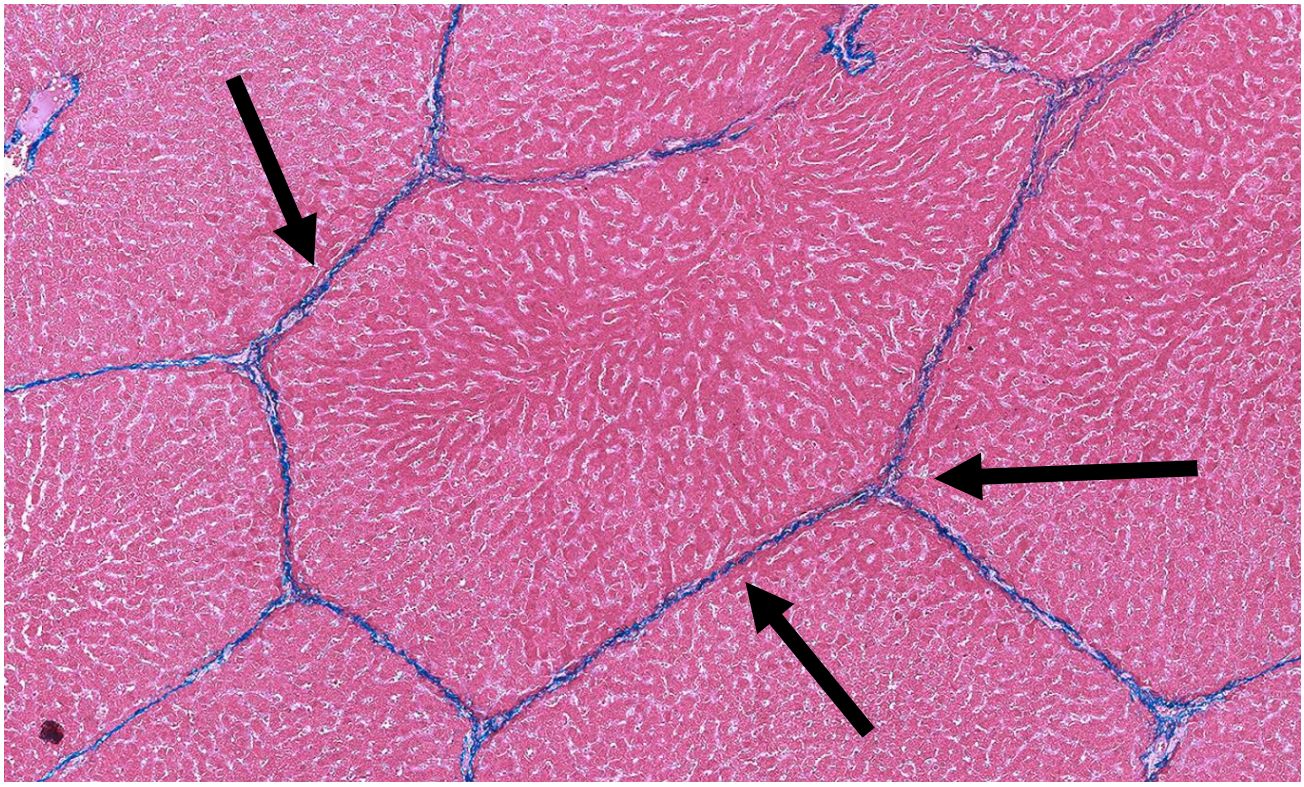

Figure 12 Representative images of Masson's trichrome stain in cohort 1 porcine liver section histologically graded for no fibrosis using porcine adapted METAVIR scheme at 5x magnification. This image shows histologically normal porcine control liver with normal preexisting fibrous septa (arrows), which impart distinct pig liver lobular architecture.

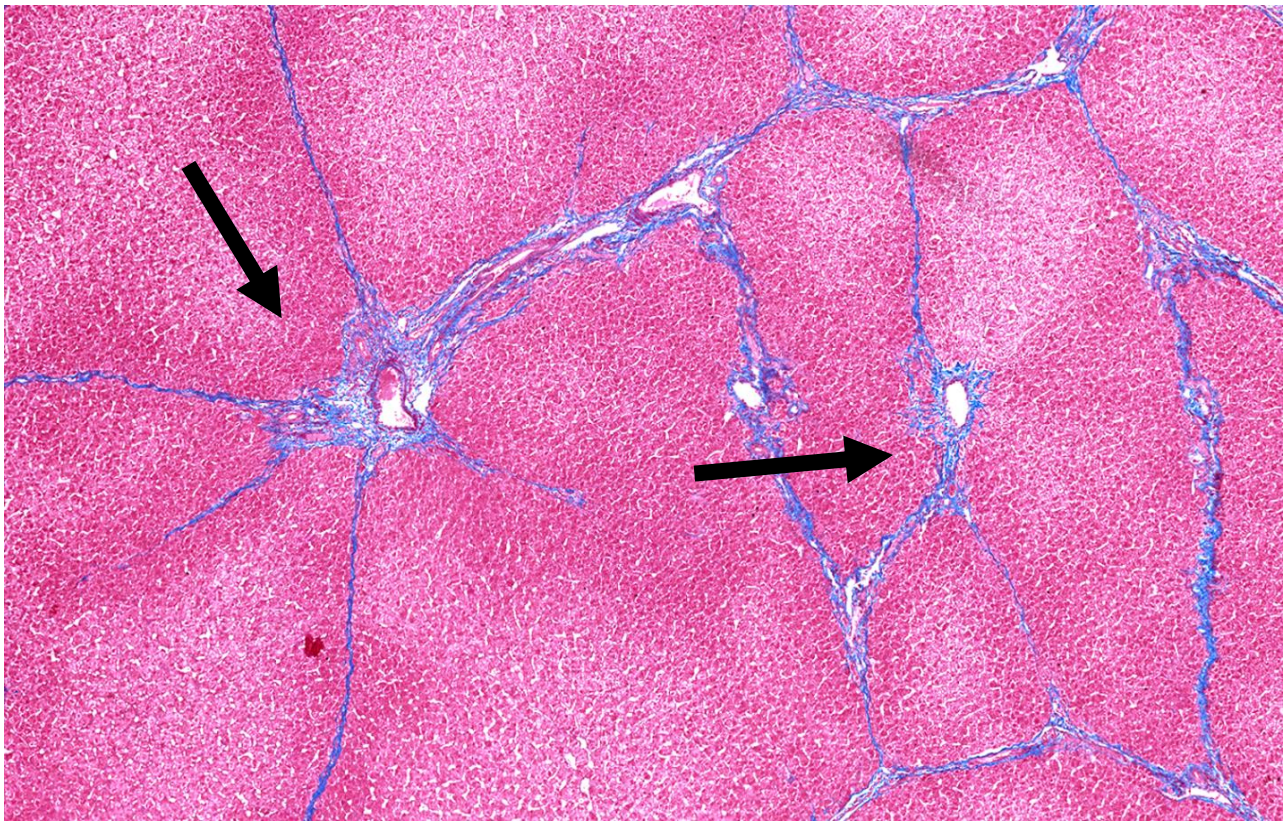

Figure 13 Representative images of Masson's trichrome stain in cohort 2 porcine liver section histologically graded for fibrosis using porcine adapted METAVIR scheme at 5x magnification. This image is of a section of biopsy taken at 20-weeks post-induction demonstrating METAVIR F2 fibrosis grading, showing significant resolution of fibrous and remodeling and reestablishment of normal lobular liver architecture, with only mild fibrous expansion of central portal areas and septa (arrows).

The presence of HE was also similarly assessed during the clinical exam for signs of cognitive dysfuntion or neurlogically-derived atacias. Swine subjects did not show a positive cross leg test at all timepoints. Functional and neurological status outcome, as assessed by food/water consumption, abnormal movements, or paralysis of any limb, with cognition assessed by alertness, response time, and overall behavior. From induction to euthanasia, no pig exhibited clinical signs of decreased food and/or water intake, abnormal ataxic movements, paralysis, or altered alertness or response time – no pig showed symptoms of HE.

V. DISCUSSION

This section will discuss the outcome of the results regarding the success of fibrosis induction, possible variations of it, and also regarding the success of fibrosis induction, with special consideration of how this model compares to the human development and progression of liver fibrosis.

a. Outcome of Fibrosis Induction

This section will review the outcome of this study in two parts: the fibrosis induction procedure, and the clinical assessment of liver fibrosis. When looking at the procedural outcome, variations in the procedure will be considered for future studies. With respect to clinical assessment of liver fibrosis, laboratory and histological outcomes will be compared to human analogues. It should be considered that a clinically analogous, but not exactly identical, disease course in the OCM is still an important model to characterize for use in translational research of fibrosis and HCC.

i. Procedure Outcome

There was successful fibrosis induction in all 10 of cohort 1 and cohort 2 experimental subjects. Peak median METAVIR score for the pooled cohorts was F3, indicating histologically-defined fibrosis. However, in experimental cohort 2, it was observed that the fibrosis achieved at 8-weeks is done so in a heterogenous pattern and is subsequently resolved to METAVIR F1 or F2 at 20-weeks. This means that while the initial toxic insult of the ethiodized oil infiltrating the liver parenchyma results in fibrosis and inflammation, there is a regeneration of the hepatocytes and therefore the effect does not persist. Therefore, this model is successful in inducing fibrosis, but the effects of it do not persist, indicating regeneration just like in normal early ALD. This may be due to variability in acquiring biopsies for histological analysis, but possible variations in the procedure can be considered to more effectively induce persistent fibrosis.

ii. Possible Variations in Procedure

This section will review some proposed variations to the fibrosis induction procedure that may result in induced fibrosis that persists to 20-weeks, or possibly longer.

The histological changes were heterogenous and regional in distribution for two main reasons: (1) the regional distribution of the lipiodol:ethanol emulsion is random and dictated by individual hepatic circulation, and (2) the infusion of the ethanol:lipiodol emulsion relies upon arterial patency while in direct contact with the toxin ethanol, which can cause vasospasm. However, the heterogenous location of fibrosis foci is not necessarily a negative feature. As a result, the experimental gross specimens were able to be utilized as samples for both normal and fibrotic liver, resulting in an internal control in addition to a control group.

The first variation to the fibrosis induction procedure that can be studied is a multiple-hit model of fibrosis induction. This study showed that the aforementioned procedure is a verified model of fibrosis induction at 8-weeks, but then resolves starting thereafter and is sub-fibrotic at 20-weeks. A fibrosis induction protocol with multiple toxic insults over an longer time course with monthly or bi-monthly hepatic artery infusions of ethanol:lipiodol emulsion has the potential to induce persistent fibrosis beyond 8-weeks. Because fibrosis was achieved at 8-weeks, it is not unreasonable to predict that a multiple-hit model of persistent liver fibrosis can be achieved still within reasonable experimental model parameters, such as less than 6 months.

Another variation of the procedure can be a change to the location of the ethanol:lipiodol infusion site. It is important to consider at which point along the hepatic artery the ethanol:lipiodol emulsion enters the hepatic circulation. This is because the point at which the ethanol:lipiodol emulsion contacts the artery, there may be vasospasm, transiently or prolonged, and the artery must remain patent-enough to permit flow-through of the emulsion, but still an appropriate caliber to prevent backflow of the infusion.

Further mitigating any vasospasm during the induction procedure, another variation may include medical dilation of hepatic vasculature before or during infusion procedure. In some experimental subjects, when the hepatic arterial wall makes contact with the ethanol:lipiodol emulsion, the hepatic artery vasospasms, thus obstructing flow and prematurely ending the infusion procedure. For these subjects, it should be considered to administer nitroglycerin or verapamil to induce local acute dilation and dilate the artery to restore flow and continue the infusion procedure. Because these medical agents utilize antagonist of arterial-wall calcium channels, this may be a technique that can be done to pre-treat the hepatic vascular pre-infusion to ensure inability to vasospasm during the infusion procedure, or if there is vasospasm, arterial caliber is still patent enough to permit flow-through and the infusion procedure can provide the flow-velocity required to move the emulsion through the liver.

The combined use of a fibrosis induction procedure as is used in this study with a high-fat diet could have the potential to accelerate the pathophysiology of fibrosis development, and more closely imitate the risk factors for liver disease. It has been shown that the combined damaging effects of heavy ethanol consumption and high dietary fat intake produces an animal model of hepatic steatosis, inflammation, and injury(Kirpich and McClain 2017). The liver disease of this combined nutritionally and locally delivered hepatic toxins, as assessed by fibrosis and cirrhosis, would provide a more clinically relevant background for developing an animal model of HCC.

III. Clinical Outcome: Interpretation of Outcome Measures

Vital signs were collected, and serum laboratory tests drawn in cohort 1 at induction and necropsy and in were drawn in cohort 2 with each biopsy and at necropsy after extended survival. While there was transient hypertension observed in some of cohort 2,

A steady climb in systolic, diastolic, and mean arterial blood pressure indicated slowly developing hypertension, most likely portal hypertension due to the fibrosis induction procedure. This is

significant because it would represent slowly increasing portal hypertension, even after there was histological resolution of fibrotic congestion in the liver. In the extended cohort 2, after the induction procedure, there was mild hypertension that persisted and worsened to severe hypertension with a mean systolic blood pressure well above 200 mmHg. It would ideal to couple these systemic blood pressure records with hepatic venous pressure gradient, to characterize and correlate systemic blood pressure changes with local hepatic pressure changes. It is known in humans that clinically relevant portal hypertension is seen after PH has been present for some time. Therefore, it would be an interesting finding to standardize that portal hypertension gradient that is diagnostic of PH in the OCM of fibrosis, but is still sub-clinically or sub-histologically apparent.

Clinical laboratory results that were significantly different in the pooled experimental cohort versus the control cohort were: glucose, BUN, and hemoglobin. While glucose was significantly decreased in the experimental cohort, there is no clinical significance to this finding because of two reasons: (1) the average serum glucose concentration was still within normal range, and (2) a random serum glucose concentration does not provide any clinical significance without a formal glucose tolerance test, which takes into account fasting serum glucose levels with temporal relation to food intake. BUN was significantly decreased in the pooled experimental group versus the control group. The decrease in BUN is still sub-clinical and within normal range for porcine BUN. Additionally, BUN in liver disease is significant when there is an increase in BUN, not a decrease. Therefore, there is no clinical significance to the decreased BUN observed in the pooled experimental cohort. Decreased average hemoglobin was observed in the experimental cohort group, but both experimental and control cohort average hemoglobin was within normal range. Therefore, perhaps this decrease in hemoglobin is indicative of very early stages of developing hepatorenal syndrome, and once fibrosis was seen to histologically resolve, so too did the detrimental effects of the

ethanol:lipiodol insult resolve systemically. It would be interesting to observe what changes in hemoglobin may be observed with the variation in the procedure mentioned above.

The histological results show that the inflammatory pattern seen in the serial biopsy analysis mimic the injurious states of hepatic damage – early inflammatory response with subsequent remodeling – which is repeated with each toxic insult in ALD. Hepatocyte damage due to ethanol exposure is the precursor to developing liver fibrosis and ultimately cirrhosis. This biochemical background of inflammation and subsequent hepatocyte regeneration as manifested by fibrosis, coupled with impaired nutrition as is often seen with alcohol dependence, combines to form a metabolic and biochemical milieu that promotes hepatocyte remodeling, hepatic failure, and neoplastic transformation in hepatocellular carcinoma. The model described in this study induced fibrosis at 8-weeks, but was subsequently resolved at 20-weeks. Because the fibrosis seen in ALD occurs over an extended period of time of cyclically repeated hepatic toxic insult, so too should the model of alcohol-induced liver fibrosis include multiple toxic insults to the liver parenchyma.

This model showed that a singular ethiodized oil infusion procedure models the toxic insult event that is cyclically repeated to result in ALD. The single toxic insult caused histologically-graded transient inflammation and fibrosis and transient elevation of laboratory indicators of compromised liver function such as hypertension and transiently elevated liver function enzymes. There was subsequent resolution of hepatocyte damage, as would occur after ceasing alcohol consumption during early stages of ALD. While the fibrosis effects where not persistent, this model does correctly mimic the ethanol toxic insult from a single instance of alcohol overuse in ALD. And because the fibrosis induction procedure delivers the ethanol toxin directly to the hepatic circulation, the multiple hits can be delivered within reasonable experimental time constraints and produce a persistent model of fibrosis – especially as a background for HCC. Therefore, this model provides a

three-point characterization of a cross-sectional-type snapshot of one instance of toxic hepatic insult.

b. Importance as Background in Developing Cancer Model of HCC

Development and refinement of experimental protocol for developing a clinically relevant model of HCC in the OCM is still being conducted. However, the relevancy of clinically relevant HCC in OCM is augmented when done in the background of liver fibrosis and cirrhosis. Therefore, this protocol for liver fibrosis induction with potential for a clinically-relevant progression to cirrhosis is key in creating the most clinically relevant version of a HCC in OCM. In an effort to develop an irreversible model of porcine fibrosis, further studies will closely mimic alcohol liver disease seen in humans in two important ways: (1) prolonged and repetitive toxic insults to liver parenchyma by using a multiple-hit model, and (2) simultaneously administering an immune antigen to catalyze immune-mediated biochemical processes involved in cirrhosis.

VI. CONCLUSION

The global public health burden of liver disease is significant and growing. The prevalence of liver cirrhosis approximates 4.5-9.5%(Graudal et al. 1991; Melato, Saso, and Zanconati 1993), affecting hundreds of millions of people worldwide. This disease accounts for approximately 2% of all global mortality, approximating 1 million deaths per year(Mokdad et al. 2014), and affects more than 600,000 persons in the United States(Scaglione et al. 2015). Among causes of liver cirrhosis, alcoholic liver disease underlies around 20% of deaths(Rehm, Samokhvalov, and Shield 2013). Not only are patients with liver cirrhosis at risk for death due to liver failure and variceal bleeding, but liver cirrhosis also increases the risk for development of primary liver cancer. Hepatocellular carcinoma results from chronic hepatic inflammation, cell necrosis, liver regeneration, and malignant transformation, with cancer developing at a 5-year incidence up to 30% in at-risk populations with liver cirrhosis(Singal and El-Serag 2016). Hepatocellular carcinoma is an aggressive malignancy that spans more than 780,000 new diagnoses while causing 750,000 annual deaths("GLOBOCAN 2012: Estimated Cancer Incidence, Mortality and Prevalence Worldwide in 2012" 2012; Flores and Marrero 2014). These staggering data highlight the urgent need for further investigation into HCC detection, development and elucidation of natural history, and response to locoregional therapy in its native comorbid cirrhotic background.

Currently established animal models for HCC have significant disadvantages, including limited recapitulation of the human condition and the protracted length of time required for model establishment. Moreover, most available models lack the mimicry of anatomic size necessary to trial new therapies targeted toward curing human disease, and small animal HCC models have meaningful deficiencies in their ability to predict clinical outcomes(Gould, Junttila, and de Sauvage 2015). Therefore, a large animal model capable of capturing a significant portion of the liver fibrosis progression to HCC continuum, that is also anatomically and physiologically analogous to human

disease course, would be a valuable resource for translation of results obtained in small animal models to human clinical practice in order to address unmet clinical needs. As HCC develops in patients with liver cirrhosis, an ideal HCC model must also be able to reflect this comorbidity and natural disease progression. The ability to concurrently induce liver fibrosis and then HCC in the OCM provides an efficient and relevant opportunity to assess the role of chronic liver disease in HCC tumorigenesis.

In this study, a previously published protocol to develop METAVIR F3-F4 fibrosis within 8-weeks in the OCM is successfully validated, demonstrating the reproducibility of this protocol across pig breeds. However, results of a prolonged time course of fibrosis induction component of this experiment indicated liver recovery, with median METAVIR grade F2 fibrosis levels at 20-weeks post-induction. While essential characteristics of the fibrotic liver biochemical micro-milieu were observed this alcohol-induced liver disease model, these results indicate that a single infusion of locally delivered lipiodol:ethanol emulsion only induces transient fibrosis with little persistence of inflammation and hepatocellular necrosis, and even less permanent remodeling of liver parenchyma. While this may represent a deficiency of the fibrosis induction procedure, this development of a multiple-hit model may more closely imitate liver fibrosis and subsequent HCC as seen in humans, because HCC clinically develops in fibrotic environments consisting of *chronic* hepatic inflammation and cellular necrosis. The liver regeneration observed in this study is consistent with the reversal of liver fibrosis observed in abstinent ALD patients presenting with pre-cirrhotic liver damage from alcohol consumption(Ismail and Pinzani 2009; Ellis and Mann 2012), with regeneration representing the microscopic reabsorption of cytoskeletal structures such as extracellular fibers and collagenous bundles(Perez-Tamayo 1979).

Overall, these results suggest prolonged or repeated exposure to alcohol is required to develop a persisting, irreversible METAVIR F4 large animal model of cirrhosis with diffuse

penetration of ethanol into the liver as an simulation of the clinically relevant cirrhotic phenotype observed in humans. Thus, the use of multiple induction procedures, a "multiple hit" model, may more closely imitate the repeated cycle of hepatocyte injury, inflammation, and repair that is required to induce extracellular matrix protein deposition and fibrogenesis(Ismail and Pinzani 2009) and observed in human liver disease. Because both cases of METAVIR F4 cirrhosis were in the 8-week sacrifice that did not experience prolonged laboratory and biopsy assessment, the results do not provide insights into the temporal durability of the cirrhosis induction procedure and whether or not the natural history of OCMs with METAVIR F4 differs from those of METAVIR F1-F3, or what temporal spacing of the fibrosis induction procedures may be necessary for a successful and persistent multiple-hit model of liver fibrosis.

While liver fibrosis was observed in 100% (10/10) of induced Oncopigs, no clinically relevant liver decompensation or laboratory changes were observed over time or in comparison to age- and gender-matched healthy control Oncopigs. This result indicates that although liver damage was successfully induced, toxic insult was not prolonged enough, therefore damage was not prolonged enough, and thus the resulting disease was not sufficiently severe, widespread, or homogeneous enough to affect measurable enzymatic activity, indicative of general liver dysfunction in the Oncopig. Our results contrast with those reported by Avritscher et al, who described occurrence of ascites in their porcine cirrhosis cohort(Avritscher et al. 2011). While seemingly discordant, these differential outcomes are in line with the concept that different individuals in the clinical setting – in this case Oncopig versus domestic pig – may manifest differential response to the same causative stress due to underlying genetic differences(Bataller, North, and Brenner 2003). It is also likely that the ethanol and ethiodized oil dose administered in our study was less than that infused in some cases of Avritscher et al, in which weight based dosing ranged from 0.60-0.95 mL/kg(Avritscher et al. 2011), while our study used 0.75mL/kg for all subjects.

The lack of diffuse disease observed both grossly and histologically in the first experimental cohort herein suggests that the temporal variations in METAVIR scores observed in the second experimental cohort is likely due to variable location of collected biopsies from liver segments with variable infusion and subsequent disease burden. To this end, core needle biopsy may not represent the optimal approach to survey fibrosis in this model given potential for disease heterogeneity and sampling error. In contrast, advanced radiologic imaging techniques, such as magnetic resonance elastography (MRE), may provide a more comprehensive view of the liver with the capacity to non-invasively diagnosis fibrosis and broadly assess the liver and liver function. In 2014, Huang et al were able to demonstrate a positive correlation between liver stiffness and histologic fibrosis in an 8 pig pilot study investigating the utility of MRE(Huang et al. 2014). Indeed, MRE has been shown to be the best qualitative assessment of fibrosis in humans(Q. B. Wang et al. 2012; Cui et al. 2017; Besa et al. 2017). This imaging modality will be incorporated in this group's future studies using the Oncopig platform.

There are limitations to this investigation. First, our study utilized the OCM as an animal model. Although this inducible cancer model has unique potential to serve as a valuable transitional bridge between small animal cancer studies and human clinical trials as it is prone to epidemiologically relevant cancers, it is not yet widely employed in preclinical investigation. Therefore, it is unknown what natural clinical course liver fibrosis may take in the OCM. This study serves as a basis to begin to establish normal values for serum laboratory values and histopathology.

Second, the sample size of Oncopigs used in this study was small. However, the information acquired was maximized by obtaining histologic, laboratory, and clinical data from all subjects, as well as including an extended time course, allowing a comprehensive clinicopathological assessment of fibrosis induction and natural history in the OCM – the first fibrosis model including all three clinically relevant components.

Third, while the dosing of the administered ethanol:lipiodol emulsion was empiric, it represented a consistent weight-based dose which allows a defined starting point for developing a relationship between administered dose and fibrosis response in future investigations.

Fourth, variation in histological results across liver biopsies, likely due to sampling variation as well as fibrosis heterogeneity, marginally confounded interpretation of fibrosis severity over time. This did, however, allow convenient and relevant internal control among animals that did experience heterogenous focal centers of cirrhosis.

Fifth, this study did not include measurement of hepatic venous pressure gradients to assess the occurrence of hemodynamic alterations associated with liver fibrosis. This may be considered in future studies.

In conclusion, this study successfully validated a protocol to develop METAVIR F3-F4 fibrosis within 8-weeks in the OCM, supporting its potential to serve as a model for HCC in a fibrotic liver background. However, repeated liver injury through a multiple-hit model for prolonged toxic insult may be required to develop an irreversible METAVIR grade F4 porcine model of cirrhosis. Future investigations will investigate whether multiple transarterial infusions of an ethanol and ethiodized oil emulsion of a longer time course will result in development of a sustained, chronic porcine model of alcohol induced liver fibrosis.

CITED LITERATURE

Abraldes, J G, M Pasarin, and J C Garcia-Pagan. 2006. "Animal Models of Portal Hypertension." *World J.Gastroenterol.* 12 (1007–9327 (Print)): 6577–84.

Allen, Bradley S., Jeffrey S. Veluz, Gerald D. Buckberg, Ernesto Aeberhard, Louis J. Ignarro, and Edward D. Verrier. 2003. "Deep Hypothermic Circulatory Arrest and Global Reperfusion Injury: Avoidance by Making a Pump Prime Reperfusate - A New Concept." *Journal of Thoracic and Cardiovascular Surgery* 125 (3): 625–32. https://doi.org/10.1067/mtc.2003.96.

Alvarez, Marco Antonio, Isabel Cirera, Ricard Solà, Ana Bargalló, Rosa Maria Morillas, and Ramon Planas. 2011. "Long-Term Clinical Course of Decompensated Alcoholic Cirrhosis: A Prospective Study of 165 Patients." *Journal of Clinical Gastroenterology* 45 (10): 906–11. https://doi.org/10.1097/MCG.0b013e3182284e13.

Ambade, Aditya, Abhishek Satishchandran, Benedek Gyongyosi, Patrick Lowe, and Gyongyi Szabo. 2016. "Adult Mouse Model of Early Hepatocellular Carcinoma Promoted by Alcoholic Liver Disease." *World Journal of Gastroenterology* 22 (16): 4091–4108. https://doi.org/10.3748/wjg.v22.i16.4091.

Avritscher, Rony, Kenneth C. Wright, Sanaz Javadi, Rajesh Uthamanthil, Sanjay Gupta, Mihai Gagea, Roland L. Bassett, Ravi Murthy, Michael J. Wallace, and David C. Madoff. 2011. "Development of a Large Animal Model of Cirrhosis and Portal Hypertension Using Hepatic Transarterial Embolization: A Study in Swine." *Journal of Vascular and Interventional Radiology* 22 (9). Elsevier Inc.: 1329–34. https://doi.org/10.1016/j.jvir.2011.04.016.

Bagnardi, V., M. Rota, E. Botteri, I. Tramacere, F. Islami, V. Fedirko, L. Scotti, et al. 2015. "Alcohol Consumption and Site-Specific Cancer Risk: A Comprehensive Dose-Response Meta-Analysis." *British Journal of Cancer* 112 (3). Nature Publishing Group: 580–93. https://doi.org/10.1038/bjc.2014.579.

Bataller, Ramón, Kari E. North, and David A. Brenner. 2003. "Genetic Polymorphisms and the Progression of Liver Fibrosis: A Critical Appraisal." *Hepatology* 37 (3): 493–503. https://doi.org/10.1053/jhep.2003.50127.

Bedossa, Pierre, and Thierry Poynard. 1996. "An Algorithm for the Grading of Activity in Chronic Hepatitis C. The METAVIR Cooperative Study Group." *Hepatology* 24: 289–93. https://doi.org/S0270913996003205 [pii]\r10.1002/hep.510240201.

Besa, Cecilia, Mathilde Wagner, Grace Lo, Sonja Gordic, Manjil Chatterji, Paul Kennedy, Ashley Stueck, et al. 2017. "Detection of Liver Fibrosis Using Qualitative and Quantitative MR Elastography Compared to Liver Surface Nodularity Measurement, Gadoxetic Acid Uptake, and Serum Markers." *Journal of Magnetic Resonance Imaging* 00 (0): 1–10. https://doi.org/10.1002/jmri.25911.

Bosch, Jaime, and Yasuko Iwakiri. 2017. "The Portal Hypertension Syndrome: Etiology, Classification, Relevance, and Animal Models." *Hepatology International*. Springer India, 1–10. https://doi.org/10.1007/s12072-017-9827-9.

Cui, Jeffrey, Elhamy Heba, Carolyn Hernandez, William Haufe, Jonathan Hooker, Michael P Andre, Mark A Valasek, et al. 2017. "MRE Is Superior to ARFI for the Diagnosis of Fibrosis in Patients with Biopsy-Proven NAFLD: A Prospective Study." *Hepatology* 63 (2): 453–61. https://doi.org/10.1002/hep.28337.MRE.

Ding, Yong fang, Zhen hui Wu, Ying jie Wei, Luan Shu, and Yun ru Peng. 2017. "Hepatic Inflammation-Fibrosis-Cancer Axis in the Rat Hepatocellular Carcinoma Induced by Diethylnitrosamine." *Journal of Cancer Research and Clinical Oncology* 143. Springer Berlin Heidelberg: 821–34. https://doi.org/10.1007/s00432-017-2364-z.

Dondorf, Felix, René Fahrner, Michael Ardelt, Eleonora Patsenker, Felix Stickel, Uta Dahmen, Utz Settmacher, and Falk Rauchfuß. 2017. "Induction of Chronic Cholestasis without Liver Cirrhosis - Creation of an Animal Model." *World Journal of Gastroenterology* 23 (23): 4191–99. https://doi.org/10.3748/wjg.v23.i23.4191.

Eliceiri, Kevin, Caroline A Schneider, Wayne S Rasband, and Kevin W Eliceiri. 2012. "NIH Image to ImageJ : 25 Years of Image Analysis HISTORICAL Commentary NIH Image to ImageJ : 25 Years of Image Analysis." *Nature Methods* 9 (7): 671–75. https://doi.org/10.1038/nmeth.2089.

Ellis, EL, and DA Mann. 2012. "Clinical Evidence for the Regression of Liver Fibrosis." *Journal of Hepatology* 56 (5): 1171–80.

Fielder, Susan E DVM. 2010. "Hematologic Reference Ranges - Appendixes - Merck Veterinary Manual." *Merck Manual- Veterinary Manual*, 5–6. http://www.merckvetmanual.com/appendixes/reference-guides/hematologic-reference-ranges.

Flores, Avegail, and Jorge A. Marrero. 2014. "Emerging Trends in Hepatocellular Carcinoma: Focus on Diagnosis and Therapeutics." *Clinical Medicine Insights: Oncology* 8: 71–76. https://doi.org/10.4137/CMO.S9926.

Forbess, Joseph M., Juan Carlos Ibla, Hart G.W. Lidov, Mark A. Cioffi, Takeshi Hiramatsu, Peter Laussen, Takuya Miura, and Richard A. Jonas. 1995. "University of Wisconsin Cerebroplegia in a Piglet Survival Model of Circulatory Arrest." *The Annals of Thoracic Surgery* 60: S494-500. https://doi.org/10.1016/0003-4975(95)00876-4.

Geerts, Anja M., Eline Vanheule, Marleen Praet, Hans Van Vlierberghe, Martine De Vos, and Isabelle Colle. 2008. "Comparison of Three Research Models of Portal Hypertension in Mice: Macroscopic, Histological and Portal Pressure Evaluation." *International Journal of Experimental Pathology* 89 (4): 251–63. https://doi.org/10.1111/j.1365-2613.2008.00597.x.

"GLOBOCAN 2012: Estimated Cancer Incidence, Mortality and Prevalence Worldwide in 2012." 2012. 2012. http://globocan.iarc.fr/Pages/fact_sheets_cancer.aspx?cancer=all.

Gould, Stephen E, Melissa R Junttila, and Frederic J de Sauvage. 2015. "Translational Value of Mouse Models in Oncology Drug Development." *Nature Medicine* 21 (5): 431–39. https://doi.org/10.1038/nm.3853.

Graudal, N., P. Leth, L. Marbjerg, and A. M. Galloe. 1991. "Characteristics of Cirrhosis Undiagnosed during Life: A Comparative Analysis of 73 Undiagnosed Cases and 149 Diagnosed Cases of Cirrhosis, Detected in 4929 Consecutive Autopsies." *Journal of Internal Medicine* 230: 165–71. https://doi.org/10.1111/j.1365-2796.1991.tb00425.x.

Hashimoto, Etsuko, Makiko Taniai, and Katsutoshi Tokushige. 2013. "Characteristics and Diagnosis of NAFLD/NASH." *Journal of Gastroenterology and Hepatology (Australia)* 28 (S4): 64–70. https://doi.org/10.1111/jgh.12271.

Hassan, Manal M., Lu Yu Hwang, Chiq J. Hatten, Mark Swaim, Donghui Li, James L. Abbruzzese, Palmer Beasley, and Yehuda Z. Patt. 2002. "Risk Factors for Hepatocellular Carcinoma: Synergism of Alcohol

with Viral Hepatitis and Diabetes Mellitus." *Hepatology* 36 (5): 1206–13. https://doi.org/10.1053/jhep.2002.36780.

Huang, Steven Y., Mohamed E. Abdelsalam, Samer Harmoush, Joe E. Ensor, Justin A. Chetta, Ken Pin Hwang, R. Jason Stafford, David C. Madoff, and Rony Avritscher. 2014. "Evaluation of Liver Fibrosis and Hepatic Venous Pressure Gradient with MR Elastography in a Novel Swine Model of Cirrhosis." *Journal of Magnetic Resonance Imaging* 39 (3): 590–97. https://doi.org/10.1002/jmri.24189.

Ikawa-Yoshida, Ayae, Saori Matsuo, Atsuhiko Kato, Yusuke Ohmori, Atsuko Higashida, Eiji Kaneko, and Masahiko Matsumoto. 2017. "Hepatocellular Carcinoma in a Mouse Model Fed a Choline-Deficient, L-Amino Acid-Defined, High-Fat Diet." *International Journal of Experimental Pathology* 98: 221–33. https://doi.org/10.1111/iep.12240.

Ismail, MH, and M Pinzani. 2009. "Reversal of Liver Fibrosis." *Official Journal of the Saudi Gastroenterology Association* 15 (1): 72–79.

Jackson, Peter, and Peter Cockcroft. 2002. "Clinical Examination of Farm Animals." In , 198–216. Oxford, United Kingdom: Blackwell Science Ltd. https://doi.org/10.1053/jevs.2002.37330.

Kim, Do Young, and Kwang-Hyub Han. 2012. "Epidemiology and Surveillance of Hepatocellular Carcinoma." *Liver Cancer* 1: 2–14. https://doi.org/10.1159/000339016.

Kirpich, Irina, and Craig McClain. 2017. "More Alcohol, More Liver Injury: Not Always True." *Alcohol and Alcoholism* 52 (6): 627–28. https://doi.org/10.1093/alcalc/agx064.

Lee, Ju-Seog. 2015. "The Mutational Landscape of Hepatocellular Carcinoma." *Clinical and Molecular Hepatology* 21 (3): 220–29. https://doi.org/10.3350/cmh.2015.21.3.220.

Li, Xiao, Xiangping Zhou, Yongsong Guan, Yi Xiang J. Wang, Diane Scutt, and Qi Yong Gong. 2006. "N-Nitrosodiethylamine-Induced Pig Liver Hepatocellular Carcinoma Model: Radiological and Histopathological Studies." *CardioVascular and Interventional Radiology* 29 (3): 420–28. https://doi.org/10.1007/s00270-005-0099-8.

Linkert, Melissa, Curtis T. Rueden, Chris Allan, Jean Marie Burel, Will Moore, Andrew Patterson, Brian Loranger, et al. 2010. "Metadata Matters: Access to Image Data in the Real World." *Journal of Cell Biology* 189 (5): 777–82. https://doi.org/10.1083/jcb.201004104.

Madoff, David C., Sanjay Gupta, Edmund P. Pillsbury, Zuxing Kan, Peggy T. Tinkey, L. Clifton Stephens, Joe E. Ensor, Marshall E. Hicks, and Kenneth C. Wright. 2007. "Transarterial versus Transhepatic Portal Vein Embolization to Induce Selective Hepatic Hypertrophy: A Comparative Study in Swine." *Journal of Vascular and Interventional Radiology* 18 (1): 79–93. https://doi.org/10.1016/j.jvir.2006.10.018.

Melato, M, F Saso, and F Zanconati. 1993. "Liver Cirrhosis and Liver Cancer. A Study of Their Relationship in 2563 Autopsies." *Zentralblatt Fur Pathologie* 139 (1): 25–30.

Mercer, K E, L Hennings, and M J J Ronis. 2015. "Biological Basis of Alcohol-Induced Cancer" 815: 185–95. https://doi.org/10.1007/978-3-319-09614-8.

Mitchell, Jennifer, Peggy T Tinkey, Rony Avritscher, Carolyn Van Pelt, Suraj Konnath George, Lianchun Xiao, Erik Cressman, et al. 2017. "Validation of a Preclinical Model of Diethylnitrosamine-Induced Hepatic Neoplasia in Yucatan Miniature Pigs" 91 (2): 90–100. https://doi.org/10.1159/000446074.Validation.

Mohapatra, Satya, Jayadeep Patra, Svetlana Popova, Amy Duhig, and Jürgen Rehm. 2010. "Social Cost of Heavy Drinking and Alcohol Dependence in High-Income Countries." *International Journal of Public Health* 55 (3): 149–57. https://doi.org/10.1007/s00038-009-0108-9.

Mokdad, Ali A., Alan D. Lopez, Saied Shahraz, Rafael Lozano, Ali H. Mokdad, Jeff Stanaway, Christopher J.L. Murray, and Mohsen Naghavi. 2014. "Liver Cirrhosis Mortality in 187 Countries between 1980 and 2010: A Systematic Analysis." *BMC Medicine* 12 (1): 1–24. https://doi.org/10.1186/s12916-014-0145-y.

Perez-Tamayo, R. 1979. "Cirrhosis of the Liver: A Reversible Disease?" *Pathology Annual* 14 Pt 2: 183–213.

Potbellied, Vietnamese, Pig Ostrich, Vietnamese Potbellied, and Pig Ostrich. 2017. "Serum Biochemical Reference Ranges - Appendixes - Merck Veterinary Manual Serum Biochemical Reference Ranges - Appendixes - Merck Veterinary Manual," 155–56.

Rehm, Jürgen, Colin Mathers, Svetlana Popova, Montarat Thavorncharoensap, Yot Teerawattananon, and Jayadeep Patra. 2009. "Global Burden of Disease and Injury and Economic Cost Attributable to Alcohol Use and Alcohol-Use Disorders." *The Lancet* 373: 2223–33. https://doi.org/10.1016/S0140-6736(09)60746-7.

Rehm, Jürgen, Andriy V. Samokhvalov, and Kevin D. Shield. 2013. "Global Burden of Alcoholic Liver Diseases." *Journal of Hepatology* 59 (1): 160–68. https://doi.org/10.1016/j.jhep.2013.03.007.

Rowe, Ian A. 2017. "Lessons from Epidemiology: The Burden of Liver Disease." *Digestive Diseases* 35 (4): 304–9. https://doi.org/10.1159/000456580.

Santhekadur, Prasanna K., Divya P. Kumar, and Arun J. Sanyal. 2017. "Preclinical Models of Nonalcoholic Fatty Liver Disease." *Journal of Hepatology*, no. October. https://doi.org/10.1016/j.jhep.2017.10.031.

Scaglione, Steven, Stephanie Kliethermes, Guichan Cao, David Shoham, Ramon Durazo, Amy Luke, and Michael L. Volk. 2015. "The Epidemiology of Cirrhosis in the United States a Population-Based Study." *Journal of Clinical Gastroenterology* 49 (8): 690–96. https://doi.org/10.1097/MCG.0000000000000208.

Schachtschneider, Kyle M, Regina M Schwind, Kwame A Darfour-Oduro, Arun K De, Lauretta A Rund, Kuldeep Singh, Daniel R Principe, et al. 2017. "A Validated, Transitional and Translational Porcine Model of Hepatocellular Carcinoma." *Oncotarget* In Press.

Schook, Lawrence B, Tiago V Collares, Wenping Hu, Ying Liang, Fernanda M Rodrigues, Laurie A Rund, Kyle M Schachtschneider, et al. 2015. "A Genetic Porcine Model of Cancer." *PloS One* 10 (7): e0128864. https://doi.org/10.1371/journal.pone.0128864.

Singal, Amit G, and Hashem B El-Serag. 2016. "Hepatocellular Carcinoma from Epidemoiology to Prevention: Translating Knowledge into Practice." *Clinical Gastroenterology and Hepatology : The Official Clinical Practice Journal of the American Gastroenterological Association* 13 (12): 1922–2013. https://doi.org/10.1080/10937404.2015.1051611.INHALATION.

Sofair, Andre N, Vaughn Barry, M Michele Manos, Ann Thomas, Atif Zaman, Norah A Terrault, Rosemary C Murphy, et al. 2010. "The Epidemiology and Clinical Characteristics of Patients with Newly Diagnosed Alcohol-Related Liver Disease: Results from Population-Based Surveillance." *Journal of Clinical Gastroenterology* 44 (4): 301–7. https://doi.org/10.1097/MCG.0b013e3181b3f760.

Sola, Ricard, Marco Antonio Alvarez, Belen Balleste, Silvia Montoliu, Monica Rivera, Mireia Miquel, Isabel Cirera, Rosa Maria Morillas, Susanna Coll, and Ramon Planas. 2006. "Probability of Liver Cancer and

Survival in HCV-Related or Alcoholic-Decompensated Cirrhosis. A Study of 377 Patients." *Liver International* 26: 62–72. https://doi.org/10.1111/j.1478-3231.2005.01181.x.

Toshikuni, Nobuyuki, Mikihiro Tsutsumi, and Tomiyasu Arisawa. 2014. "Clinical Differences between Alcoholic Liver Disease and Nonalcoholic Fatty Liver Disease." *World Journal of Gastroenterology* 20 (26): 8393–8406. https://doi.org/10.3748/wjg.v20.i26.8393.

Wang, Lin, Jun Zhou, Shengmin Yan, Guangsheng Lei, Chao Hung Lee, and Xiao Ming Yin. 2017. "Ethanol-Triggered Lipophagy Requires SQSTM1 in AML12 Hepatic Cells." *Scientific Reports* 7. Springer US: 1–13. https://doi.org/10.1038/s41598-017-12485-2.

Wang, Qing Bing, Hui Zhu, Hai Ling Liu, and Bei Zhang. 2012. "Performance of Magnetic Resonance Elastography and Diffusion-Weighted Imaging for the Staging of Hepatic Fibrosis: A Meta-Analysis." *Hepatology* 56 (1): 239–47. https://doi.org/10.1002/hep.25610.

Wu, Jian. 2016. "Utilization of Animal Models to Investigate Nonalcoholic Steatohepatitis-Associated Hepatocellular Carcinoma." *Oncotarget* 7 (27): 42762–76. https://doi.org/10.18632/oncotarget.8641.

Xin, Bo, Ying Cui, Yanxia Wang, Lei Wang, Jipeng Yin, Licheng Zhang, Hailin Pang, Helong Zhang, and Rui An Wang. 2017. "Combined Use of Alcohol in Conventional Chemical-Induced Mouse Liver Cancer Model Improves the Simulation of Clinical Characteristics of Human Hepatocellular Carcinoma." *Oncology Letters* 14 (4): 4722–28. https://doi.org/10.3892/ol.2017.6800.

Yang, Alice L. 2008. "Epidemiology of Alcohol-Related Liver and Pancreatic Disease in the United States." *Archives of Internal Medicine* 168 (6): 649. https://doi.org/10.1001/archinte.168.6.649.

VITA

NAME: Nasya Mendoza-Elias

EDUCATION

University of Illinois at Chicago College of Medicine *Chicago, IL*
Doctor of Medicine *Expected May 2018*
University of Illinois at Chicago College School of Public Health *Chicago, IL*
Master of Science – Clinical and Translational Science *Expected May 2018*
"Porcine Model of Liver Fibrosis: clinical, laboratory, and histological correlate of human disease"
The University of Chicago *Chicago, IL*
Bachelor of Science – Biology with Specialization in Neuroscience June 2012

AWARDS AND ACHIEVEMENTS

Selected Professions Fellowship Grant *Washington, DC*
American Association of University Women (AAUW) April 2017
Interventional Radiology Research Fellowship *Chicago, IL*
UIC Hospital, Dept of Radiology/ UIC College of Medicine July 2016 - *present*
Medicina Fellows Research Scholarship *Chicago, IL*
UIC Hispanic Center of Excellence May – August 2014
Student Travel Award for FENS Forum 2010 *Amsterdam, Netherlands*
Federation of European Neuroscience Societies (FENS) July 2010
University Scholar *Chicago, IL*
University of Chicago September 2007 – June 2012

RESEARCH EXPERIENCE

University of Illinois Hospitals/University of Illinois at Chicago College of Medicine *Chicago, IL*
Division of Interventional Radiology, Ron Gaba, MD May 2016 – present
· IR clinical studies of retro- and prospective clinical outcomes, locoregional therapy outcomes, and translational studies using large animal models for human comparison and associated proteomics
University of Illinois at Chicago *Chicago, IL*
Dept. of Neurology, Jeffrey A. Loeb, MD, PhD, Qin Li Jiang, MD, PhD 2014 – 2015
· Morphology/gene expression changes in human ALS muscle; on-call rapid tissue collection team
Rosalind Franklin University of Medicine and Science *North Chicago, IL*
Dept. of Neuropharmacology, Dean Gloria Meredith, PhD & David Rademacher, PhD 2009 – 2013
· Research assistant and lab manager analyzing anatomic morphologic changes in rat model of L-DOPA induced dyskinesias and drug-addiction memory
University of Chicago *Chicago, IL*
Dept. of Neurobiology, Peggy Mason, PhD and Kevin Hellman, PhD 2008 – 2009
· Research Assistant investigating the role of the raphe magnus role in homeostasis via mouse electrophysiology recordings and behavioral studies
Northwestern School of Medicine/University of Chicago *Chicago, IL*
Northwestern Memorial Hospital Radiology, David Channin, MD Summer 2008
· MedIX Internship; codifying imaging protocols for RadLexicon
·

PUBLISHED MANUSCRIPTS

Morrison JD, **Mendoza-Elias N**, Lipnik AJ, Lokken RP, Bui JT, Ray CE, Gaba RC. "Gastric Varices Bleed at Lower Portosystemic Pressure Gradients than Esophageal Varices." Journal of Vascular and Interventional Radiology, 17 Jan. 2018, doi:10.1016/j.jvir.2017.10.014.

Mendoza-Elias N, Shakur SF, Charbel FT, Alaraj A. (2017) Cerebral arteriovenous malformation draining vein stenosis is associated with atherosclerotic risk factors. J NeuroIntervent Surg. 2017 Nov; 0:1–3

Schachtschneider KM, Schwind RM, Newson J, Kinachtchouk N, Rizko M, **Mendoza-Elias N**, et al. (2017) The Oncopig Cancer Model: An Innovative Large Animal Translational Oncology Platform. *Front. Oncol.* 2017 Jun; 7:190

Gaba R, **Mendoza-Elias N**, Morrison JD, Valeshabad AK, Lipnik AJ. (2016) Decision-making for Selection of Transarterial Locoregional Therapy of Metastatic Neuroendocrine Tumors. Seminars in Interventional Radiology. 2017 June; 34(2): 101-108.

Ahir BK, **Mendoza-Elias N**, Lakka SS. (2017) SPARC overexpression alters microRNA expression profiles involved in tumor progression. Genes and Cancer. 2017 Jan; 8(1-2): 453-471.

Rademacher DJ, **Mendoza-Elias N**, Meredith GE. (2014) Effects of context-drug learning on synaptic connectivity in the basolateral nucleus of the amygdala in rats. Eur J Neurosci. 2015 Jan; 41(2): 205-15.

Zhang Y, Meredith GE, **Mendoza-Elias N**, Rademacher DJ, Yuan-Tseng K, Steece-Collier K. (2012) Aberrant Restoration of Spines and their Synapses in L-dopa-Induced Dyskinesia: Involvement of Corticostriatal but not Thalamostriatal Synapses. Journal of Neuroscience. 2013 Jul; 33(28): 11655-67.

PUBLICATIONS – *ACCEPTED FOR PUBLICATION*

Mendoza-Elias N, Gaba R (2018) MELD Score does not Underestimate Short-term Mortality Risk in Women versus Men after TIPS Creation. CardioVascular and Interventional Radiology. CVIR-D-18-00104.

Gaba RC, **Mendoza-Elias N**, Regan DP, Garcia KD, Lokken RP, Schwind RM, Eichner M, Thomas FM, Rund LA, Schook LB, Schachtschneider KM. Characterization of an inducible alcoholic liver fibrosis model for hepatocellular carcinoma investigation in a transgenic porcine tumorigenic platform. J Vasc Interv Radiol.

Shakur SF, Alaraj A, **Mendoza-Elias N**, Osama M, Charbel FT (2017) Hemodynamic characteristics associated with cerebral aneurysm formation in patients with carotid occlusion. JNS17-1794.

Gaba RC, **Mendoza-Elias N**, Schilling JH, Lipnik AJ. Balloon-occluded transvenous obliteration for gastric varices. In: Keefe NA, Haskal ZJ, Park AW, and Angle JF, eds. IR Playbook: A Comprehensive Introduction to Interventional Radiology. Springer.

ORAL PRESENTATIONS

Schachtschneider KM, **Mendoza-Elias N**, Regan DP, Garcia KD, Rund LA, Schook LB, Gaba RC (29017) Characterization of an inducible alcoholic liver fibrosis model for hepatocellular carcinoma investigation in a transgenic porcine platform. Poster presentation. American Association for Cancer Research (AACR) 2018 Annual Meeting, Chicago IL, 4/16/2018

Mendoza-Elias N, Morrison J, Lipnik A, Lokken R, Bui J, Ray C, Gaba RC (2017) MELD Score does not Underestimate Short-term Mortality Risk in Women versus Men after TIPS Creation. Oral Presentation. Soc of Interv Radiology (SIR) 2017 Annual Meeting, Washington DC, 3/8/2017

Morrison JD, **Mendoza-Elias N**, Lipnik AJ, Lokken RP, Bui JT, Ray CE, Gaba RC (2017) Gastric varices bleed at lower portosystemic pressure gradients than esophageal varices. Oral presentation. Soc of Interv Radiology (SIR) 2017 Annual Meeting, Washington DC, 3/8/2017

Mendoza-Elias N (2012) The significance of plasticity in thalamostriatal synapsis in Levodopa Induced Dyskinesias. Chicago-Area Undergraduate Research Symposium (CAURS) 2012, Chicago, IL, 3/3/2012

ABSTRACTS AND POSTERS

Mendoza-Elias N, Shakur SF, Charbel FT, Alaraj A (2017) Cerebral Arteriovenous Malformation Draining Vein Stenosis Is Associated with Atherosclerotic Risk Factors. Congress of Neurological Surgeons (CNS) 2017 Annual Meeting

Mendoza-Elias N, Morrison J, Lipnik A, Lokken R, Bui J, Ray C, Gaba R (2017) MELD Score does not Underestimate Short-term Mortality Risk in Women versus Men after TIPS Creation. Soc for Interv Radiology (SIR) Abst

Shakur SF, Alaraj A, **Mendoza-Elias N**, Osama M, Charbel FT (2017) Hemodynamic Characteristics Associated with Cerebral Aneurysm Formation In Patients With Carotid Occlusion. CNS 2017 Annual Meeting Abst

Morrison J, **Mendoza-Elias N**, Lipnik A, Lokken R, Bui J, Ray C, Gaba R (2017) Gastric Varices Bleed at Lower Portosystemic Pressure Gradients than Esophageal Varices. Soc for Interv Radiology (SIR) Abst

Mendoza-Elias N (2015) Neurosurgery Case Report on Endovascular Aneurysm Coiling. 2015 UIC COM Annual Mentors Program Symposium Abst

Mendoza-Elias N, Meredith GE, Zhang Y, Rademacher D, Steece-Collier K (2012) Structural plasticity of thalamostriatial synapses in a model of levodopa-induced dyskinesias. Soc for Neuroscience (SfN) Abst

Mendoza-Elias N, Meredith GE, Zhang Y, Rademacher D, Steece-Collier K (2012) Structural plasticity of corticostriatal synapses in a model of levodopa-induced dyskinesias. Soc for Neuroscience (SfN) Abst

Zhang Y, Meredith GE, **Mendoza-Elias N**, Rademacher, Steece-Collier K (2012) Neural Plasticity of Corticostriatal and Thalamostriatal Synapses in a Model of Levodopa-Induced Dyskinesias. The Am Soc for Neural Therapy and Repair Abst

Rademacher DJ, Rosenkranz JA, Hetzel A, **Mendoza-Elias N**, Meredith GE (2012) Amphetamine-associated contextual learning produces a constellation of structural plastic changes of synapses in basolateral amygdala circuitry. Soc for Neuroscience (SfN) Abst

Mendoza-Elias N, Rademacher D J, Meredith G E (2010) Context-drug learning increases the number of synapses in the basolateral amygdala. Federation of European Neuroscience Societies (FENS) Forum Abst

Hetzel A, **Mendoza-Elias N**, Rademacher DJ, Meredith GE, Rosenkranz JA (2010) Amphetamine place conditioning leads to increased spontaneous synaptic events in the basolateral amygdala in vitro. Soc for Neuroscience (SfN) Abst

Zhang Y, **Mendoza-Elias N**, Steece-Collier K, Meredith GE (2010) Ultrastructural study of striatal synapses in a rat model of L-DOPA-induced dyskinesias. Soc for Neuroscience (SfN) Abst

ADMINISTRATIVE ACTIVITIES

Promotions Committee	*UIC COM, Chicago, IL*
Student Representative	2013 – 2017
Curricular Student Education Team (SET) Committee Representative	*UIC COM, Chicago, IL*
M1/M2 Rep, M2/M3 Rep, M3-transition	2013 – 2016
Student Curricular Board (SCB) Representative	*UIC COM, Chicago, IL*
M3-transition, M4	2016 – 2018

ORGANIZATION MEMBERSHIPS	SINCE
American Association of Neurological Surgeons (AANS)	2013
American Medical Association (AMA)	2013
Chicago Medical Society (CMS)	2013
Congress of Neurological Surgeons (CNS)	2014
Latino Medical Students Association (LMSA)	2014
Society of Interventional Radiology (SIR)	2016
Society for Neuroscience (SfN)	2009
Society of NeuroInterventional Surgery (SNIS)	2017
Student National Minority Association (SNMA)	2015

VOLUNTEERING, HEALTH ADVOCACY, AND EXTRACURRICULAR ACTIVITIES

UIC Health Associated Latino Association (HOLA) Suture Workshop	*Chicago, IL*
College of Medicine tutor	2015 – present
LMSA Regional Mid-West Conference	*Cincinnati, OH*
Policy Advocate Exhibitor	Feb 26 – 27, 2016
PNHP National Conference	*Chicago, IL*

Leadership Academy/Student Travel Awardee — Oct 30 – Nov 1, 2015

SNMA Region II Conference — *Maywood, IL*

Member/Policy Advocate — October 3, 2015

Illinois Heart Rescue (ILHR) — *Chicago, IL*

AED Trainer/Policy Advocate — Aug 2014 – June 2016

ALS Association Education Scientific Symposium – University of Chicago — *Chicago, IL*

Researcher and Participant — October 2014

Medicina Scholars – UIC Hispanic Center of Excellence — *Chicago, IL*

Student Mentor — Spring 2014 – present

Summer Prematriculation Program — *Chicago, IL*

Anatomy Tutor and Dissector — May – June 2014

Surgery Exploration and Discovery (SEAD) Program - UI, Dpt of Surgery — *Chicago, IL*

Participant — May 2014

Medicina Academy Apprentice Program – UIC Hispanic Center of Excellence — *Chicago, IL*

Neuroscience Tutor — April 2014

Parkinson's Disease Mini-Course – Rosalind Franklin University — *North Chicago, IL*

Participant — Jan 2010

EMPLOYMENT

UIC College of Medicine, Urban Health Program — *Chicago, IL*

Peer Educator — June 2014 – 2015

MyGuru Tutoring — *Chicago, IL*

Tutor — January 2013 –2018

SKILLS

Research Skills:

Clinical statistical analysis and database management
Electron microscopy tissue processing and micrograph acquisition
Immunohistochemistry for light and fluorescent microscopy
qPCR, Southern blot, Western blot
Animal model experience: rodent, swine

Languages:

Spanish (fluent), Hebrew (beginner), Arabic (beginner)